


8-2014

DISCOVERY AND ELUCIDATION OF THE FGFR3-TACC3 RECURRENT FUSION IN GLIOBLASTOMA

Brittany C. Parker Kerrigan

Follow this and additional works at: http://digitalcommons.library.tmc.edu/utgsbs_dissertations

 Part of the [Biology Commons](#), [Genomics Commons](#), [Medicine and Health Sciences Commons](#), and the [Other Neuroscience and Neurobiology Commons](#)

Recommended Citation

Parker Kerrigan, Brittany C., "DISCOVERY AND ELUCIDATION OF THE FGFR3-TACC3 RECURRENT FUSION IN GLIOBLASTOMA" (2014). *UT GSBS Dissertations and Theses (Open Access)*. Paper 509.

This Dissertation (PhD) is brought to you for free and open access by the Graduate School of Biomedical Sciences at DigitalCommons@The Texas Medical Center. It has been accepted for inclusion in UT GSBS Dissertations and Theses (Open Access) by an authorized administrator of DigitalCommons@The Texas Medical Center. For more information, please contact laurel.sanders@library.tmc.edu.

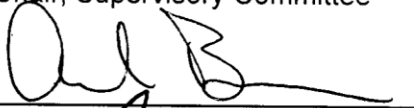
DISCOVERY AND ELUCIDATION OF THE FGFR3-TACC3 RECURRENT FUSION IN
GLIOBLASTOMA

By
Brittany Candies Parker Kerrigan, B.S.

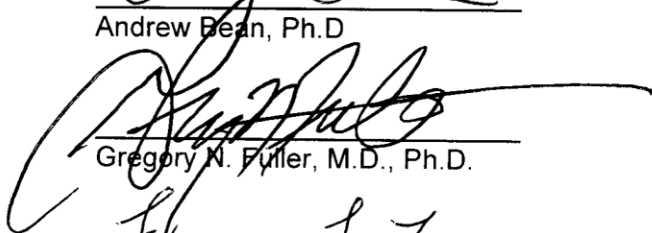
APPROVED:



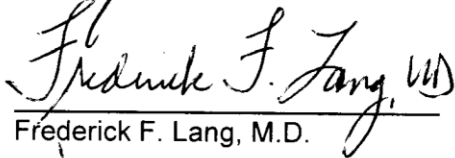
Wei Zhang, Ph.D.
Chair, Supervisory Committee



Andrew Bean, Ph.D



Gregory N. Fuller, M.D., Ph.D.



Frederick F. Lang, M.D.



Kartik Venkatachalam, Ph.D.

APPROVED:

Dean, The University of Texas
Graduate School of Biomedical Sciences at Houston

**DISCOVERY AND ELUCIDATION OF THE FGFR3-TACC3 RECURRENT FUSION IN
GLIOBLASTOMA**

A

DISSERTATION

Presented to the faculty of
The University of Texas
Health Science Center at Houston
and
The University of Texas
MD Anderson Cancer Center
Graduate School of Biomedical Sciences
in Partial Fulfillment
of the Requirements
for the Degree of

DOCTOR of PHILOSOPHY

by

Brittany Candies Parker Kerrigan, B.S.

Houston, TX

August 2014

Dedication

I dedicate this dissertation to Yong Park, who is the reason why I chose a career path in research.

Acknowledgments

I thank my Ph.D. advisor, Dr. Wei Zhang for allowing me to join his lab. Dr. Zhang taught me how to “think outside the box,” and to never stop trying. Dr. Zhang encouraged me to be the best scientist I could be and helped open the door for unbelievable opportunities. I will never forget his motivational speeches before lab meeting, and I will always have his words in the back of my mind, to wherever life takes me: “Be the shark!”

I also want to thank Dr. Andrew Bean, an absolutely incredible mentor, who from the beginning believed in me and offered solace and advice no matter what I threw his way. I will never forget the tremendous stress I felt while planning for my qualifying exam, and how comforting and calming Dr. Bean was, who diminished my fears just enough to earn that unconditional pass. Dr. Bean takes the time to listen, and he cares about what students need in order to succeed during their graduate career. Balancing both a career in administration and science, Dr. Bean shows what it takes to become a well-rounded, successful scientist. Dr. Bean became more than a mentor to me, but a family friend. I am confident that I speak on behalf of the students and faculty at UT-GSBS when I say we are extremely blessed to have Dr. Bean on our team. I thank Dr. Gregory Fuller, whose constant smile and energy could immediately fill you with joy and motivation. Dr. Fuller’s passion for science and medicine was addicting, and motivated me to jump into my scientific career with as much rigor as he had. Dr. Fuller is a tremendous source of encouragement and is truly an inspiration. There is a reason why I went to Dr. Fuller for a “pep” talk before my first postdoctorate fellowship interview. He made me feel extremely confident, which helped me earn the position. I am absolutely indebted to Dr. Fuller for all of his help and support throughout my graduate school career. I also want to thank Dr. Frederick Lang and Dr. Kartik Venkatachalam for their guidance and point of view while preparing for my Ph.D. defense. I am so excited to begin the next step in my journey working under Dr. Lang and am very grateful that he agreed to take me on as a postdoctorate fellow. Dr. Venkatachalam’s sense

of excitement and energy for science is addicting and his ideas for my project were extremely helpful. I am extremely grateful for this incredible group of mentors who have helped me grow as an independent scientist over the past five years.

I am absolutely indebted to UT GSBS for accepting me into their program. This graduate school is incredibly supportive of its students, from the administration to the faculty members. I am extremely blessed to have been part of such an amazing institution.

I would not be here if it was not for my parents, Steven and Barbara Parker. My father always taught me that if you want to be successful, you must put in 110%. He would calm my nerves when school got tough by comparing my journey to his as a “young accountant.” He was always there to listen to my worries, and to offer advice. He also would take me on fishing trips that would immediately take away any fear I had; one of the pastimes I loved the most with my father. I also want to thank my mother, who taught me the perseverance it takes to succeed. She encouraged me to become a strong, independent woman, who accomplishes her dreams no matter what it takes. She always was willing to lend an ear, or a delicious dinner, when my research got tough. My mother is my biggest role model, as she exemplifies what it means to be a devoted wife and mother while running an extremely successful business that she started from nothing. My mother taught me how to make a house a home, and how to never back down, no matter how tough life becomes.

I also want to thank my brother, Stevie Parker, who always believed in me, and loved to brag behind my back to his friends “my sister is a brain doctor.” He always encouraged me when I would call to give news of an award, or a talk I was invited to give. I also want to thank my extended family, especially my Aunt Trudie Underwood for your love and support. Hearing her say “I am so proud of you, little darlin’” could calm anyone’s nerves. I couldn’t have done any of this without the love of my family.

I want to thank my husband, Ryan Kerrigan, and for his continuous encouragement when the going got tough. I love his famous quote from his grandfather, “Get up, you’re

winning!” His work ethic encouraged me to work equally as hard and ability to get through tough situations was inspiring. I am so lucky to have met such an incredible man to be by my side throughout this journey. Upon marrying Ryan, I also gained a new family. I will never forget the support and love given to me by my new sisters in Hilton Head upon news that our manuscript was scooped. I feel so blessed to have become part of such an amazing family. I feel truly proud to say that I am a “Kerrigan.”

I am extremely grateful to have such amazing friends. Yong Park got my foot in the door in the respected neuroscientist Dr. Lynch’s lab. Yong’s constant love, support, and encouragement have been my backbone throughout the past five years and for that I am extremely grateful. I was not born with a sister, but gained one when I met Dr. Kari Brewer Savannah. Dr. Savannah is not only an incredible friend, but also a role model in my life and for many other young women scientists. She encouraged me when the going got tough, and always had constructive advice to provide. I am extremely grateful for this friendship.

I don’t look at the people who work in the lab with me as peers; I see them as my family. They are the people who helped me, supported me, taught me, and were the first to make me laugh when an experiment failed or I was turned down for an award. From Dave’s constant badgering and therapeutic life advice, to giggling across my lab bench with Corrine “Ricey”, to home ownership discussions with Dr. Moore and gardening topics with Dr. Hu. I thank Dr. Kristen Turner for introducing me to the Zhang lab, and for being an incredible source of support and wisdom throughout my Ph.D. career. I thank Lalit Patel for offering hours of his time to help prepare me for oral presentation competitions and for helping raise my confidence to take the proverbial “bull by its horns.” I have also gotten to get to know and learn from several coworkers outside of Texas, including Matti Annala, Manon Engels, Krissie Lenting, and Drs. Kexin Chen, Lina Zhang, Xia Li, Guoyan Liu, Yan Sun, Jing Wen, Kirsi Granberg, Ilya Schmulevich, and Tao Chen. I feel so lucky to be a part of such an amazing group of people. I thank you all for your help, support, and encouragement.

Abstract

Fusion genes occur due to chromosomal instability where two previously separate genes rearrange and fuse together, forming a hybrid gene. The first fusions were reported in leukemias; however, with the advent of more powerful sequencing technologies, fusions have recently been reported in several solid tumors. Using next-generation deep sequencing approaches, we discovered a fusion gene connecting the *fibroblast growth factor receptor 3 (FGFR3)* gene to the *transforming coiled-coil containing protein 3 (TACC3)* gene in glioblastoma multiforme. The fusion occurred in 8.3% of patient samples, but not in low grade or normal samples. *FGFR3-TACC3* produced an in-frame fusion protein that promoted an oncogenic phenotype both *in vitro* and *in vivo*. While the fusion was overexpressed and contained the majority of the *FGFR3* gene, levels of wild-type *FGFR3* were very low. We attributed this effect to the ability of the fusion to bypass miR-99a regulation, by losing the 3' UTR of *FGFR3* upon formation of the fusion. The fusion activated ERK and STAT3 signaling, and was more sensitive to FGFR, ERK, and STAT3 inhibitors, while more resistant to treatment with frontline chemotherapy agent, temozolomide.

Table of Contents

Dedication	iii
Acknowledgements	iv
Abstract	vii
Table of Contents	viii
List of Figures.....	x
List of Tables.....	xi
List of Abbreviations	xii
Chapter 1: Introduction	14
1.1 The Central Nervous System	14
1.2 Gliomas	15
1.3 Fusion genes	21
1.4 Fibroblast Growth Factor Receptor (FGFR) Family	30
1.5 Transforming Acidic Coiled-Coil Containing Protein 3 (TACC3)	31
Chapter 2: Materials and methods	33
Chapter 3: Results	46
3.1 The <i>FGFR3-TACC3</i> fusion gene occurs in 8.3% of glioblastoma patients	46
3.2 The <i>FGFR3-TACC3</i> fusion escapes microRNA regulation	52
3.3 The <i>FGFR3-TACC3</i> fusion activates ERK and STAT3 signaling.....	58
3.4 The <i>FGFR3-TACC3</i> fusion exhibits an oncogenic phenotype <i>in vitro</i>	60
3.5 The <i>FGFR3-TACC3</i> fusion is oncogenic <i>in vivo</i>	63

3.6	The <i>FGFR3-TACC3</i> fusion localizes to the nucleus	66
3.7	The <i>FGFR3-TACC3</i> fusion is activated by bFGF ligand.....	68
3.8	The <i>FGFR3-TACC3</i> fusion is chemoresistant	70
3.9	The <i>FGFR3-TACC3</i> fusion is sensitive to targeted therapy.....	71
Chapter 4: Summary		74
Chapter 5: Discussion.....		75
5.1	FGFR family fusions genes know no cancer boundaries.....	75
5.2	The <i>FGFR3-TACC3</i> fusion is an oncogenic driver event in GBM.....	77
5.3	The <i>FGFR3-TACC3</i> fusion escapes miR-99a regulation.....	79
5.4	Therapeutic implications of targeting <i>FGFR3-TACC3</i> fusions	81
Chapter 6: Future directions		83
6.1	Elucidating the oncogenic result of losing the C-terminal of FGFR3.....	83
6.2	Determine key phosphorylation sites on <i>FGFR3-TACC3</i>	84
6.3	Elucidating therapeutic options for <i>FGFR3-TACC3</i> patients <i>in vivo</i>	85
Bibliography		87
Vita		108

List of Figures

Figure 1. The molecular structure of TMZ	21
Figure 2. Fusion discovery coincides with sequencing technology	26
Figure 3. Locations of fusion genes that occur in solid tumors	27
Figure 4. Mechanisms of fusion gene formation.....	28
Figure 5. Fusion filtering algorithm	47
Figure 6. Breakdown of fusion candidate discovery	48
Figure 7. FGFR3-TACC3 fusion validation.....	50
Figure 8. FGFR3-TACC3 fusion forms an in frame fusion protein	51
Figure 9. miR-99a is overexpressed and targets FGFR3 in GBM.	54
Figure 10. The FGFR3-TACC3 fusion escapes miR-99a regulation.....	56
Figure 11. Of highest GBM miRNA, only miR-99a targets FGFR3	57
Figure 12. FGFR3-TACC3 promotes ERK and STAT3 activity	59
Figure 13. FGFR3-TACC3 is oncogenic <i>in vitro</i>	62
Figure 14. FGFR3-TACC3 is tumorigenic <i>in vivo</i>	65
Figure 15. FGFR3-TACC3 is localization	67
Figure 16. FGFR3-TACC3 is activated by bFGF ligand treatment.	69
Figure 18. FGFR3-TACC3 is chemoresistant.....	70
Figure 19. FGFR3-TACC3 is sensitive to targeted therapy	73
Figure 20. Summary	74
Figure 21. FGFR family fusions in a wide array of solid tumors.....	76
Figure 22. Reported oncogenic phenotypes of FGFR family fusions.....	79
Figure 23. The <i>FGFR3-TACC3</i> fusion escapes miR-99a regulation in GBM.....	81

List of Tables

Table 1. The World Health Organization glioma grading system..... 16

Table 2. Fusion genes and their methods of discovery.23

Abbreviations

CNS	central nervous system
GBM	glioblastoma multiforme
WHO	World Health Organization
PTEN	phosphatase and tensin homolog
TP53	tumor protein 53
MDM2	murine double minute 2
RB	retinoblastoma
CDK	cyclin dependent kinase
RTK	receptor tyrosine kinase
EGFR	epidermal growth factor receptor
PGFR	platelet-derived growth factor receptor
EBRT	external beam radiation therapy
TMZ	temozolomide
MGMT	O6-methylguanine-DNA methyltransferase
Bcl	B-cell lymphoma
CML	chronic myeloid leukemia
BCR	breakpoint cluster region
ABL1	abelson murine leukemia viral oncogene homolog 1
PCR	polymerase chain reaction
FISH	fluorescent <i>in situ</i> hybridization
UTR	untranslated region
IGF-1R	insulin-like growth factor 1 receptor
FGFR	fibroblast growth factor receptor
Ig	immunoglobulin

TACC3	transforming acidic coiled-coil containing protein 3
RMA	robust multiarray analysis
DAB	diaminobenzidine
TCGA	The Cancer Genome Atlas
IPA	Ingenuity Pathway Analysis
MET	hepatocyte growth factor receptor

CHAPTER 1: Introduction

1.1 The Central Nervous System

The Central Nervous System (CNS) is comprised of the brain and spinal cord. The brain serves many important functions, including controlling thought, movement, speech, memory, and regulation of internal organs throughout the body. Specialized structures within the brain can perform specific tasks. For example, the cerebellum at the back of the brain is responsible for fine-tuning motor activity and equilibrium. On the other hand, the cerebrum, which forms the majority of the brain, is involved in controlling memory, sensation, vision, and hearing, among other important functions.

The brain is comprised of two major cell types: neurons and glial cells. Neurons are responsible for transmitting electrical information from neuron to neuron, across a small space called the synapse. This electrical information is transmitted by the release of small chemical messengers across the synapse, known as neurotransmitters. The average neuron consists of a round cell body that contains the soma where the nucleus is located. Projections extend out from the cell body, which make up the dendrites. The cell body is then connected to a long structure called an axon, finally terminating at the axon terminal – the location where neurotransmitters are released. However, neurons exist in varying shapes and sizes depending on their function and location in the brain and peripheral nervous system. Neurons can range in size from microscopic dimensions to extending up to a meter long and can vary widely in structure.

Glial cells, from the Greek word meaning “glue”, outnumber neurons by 50 glial cells to every one neuron. Glial cells are referred to as “neural helper cells,” and differ from neurons in that they can divide, while neurons are post-mitotic cells. Astrocytes are the most abundant cell type in the brain and are responsible for clearing excess neurotransmitter from the synaptic cleft of firing neurons, in order to prevent neuronal excitotoxicity, or

overactivation of a neuron. They are also involved in supplying important nutrients to neurons. Oligodendrocytes are responsible for the myelination of the axons of neurons, which allows for rapid transmission of information along the axon to the nerve terminal.

1.2 Gliomas

Gliomas are tumors of the brain and spinal cord, and exhibit poor patient prognosis. Glioma accounts for 31% of all primary CNS tumors, and 80% of all malignant primary CNS tumors (Central Brain Tumor Registry of the United States <http://www.CBTRUS.org>). Current treatment regimens yield meager benefit, as patients with high grade, invasive glioma, known as glioblastoma (GBM), typically do not survive longer than a year following diagnosis (Stupp et al, 2009b). Approximately 18,000 new glioma cases will arise every year in the US, which will result in 13,000 deaths on average (Central Brain Tumor Registry of the United States <http://www.CBTRUS.org>).

Gliomas are named by which cell type they resemble. For example, ependymoma arise from ependymal cells, astrocytomas from astrocytes, oligodendrogliomas from oligodendrocytes, etc. Gliomas can also be named by the location in the brain in which they occur. For example, optic nerve gliomas occur within the pregeniculate optic pathway, while brainstem gliomas occur in the brainstem. Gliomas can further be categorized upon which area of the brain they arise from – supratentorial glioma occur in the cerebrum, and comprise the majority of adult gliomas while infratentorial gliomas occur in the cerebellum and comprise most childhood gliomas.

The World Health Organization (WHO) grades glioma on a scale from one to four, where grade four glioma confer the worst prognosis (Table 1). Grade I gliomas include pilocytic astrocytoma and subependymal giant cell astrocytoma, while Grades II-IV include diffuse glioma. The mean age of diagnosis varies according to glioma subtype. For example, on average pilocytic astrocytoma patients are 17 years old, while GBM, the most deadly

form of glioma, confers a median age of diagnosis of 62 years old (Ohgaki, 2005; Ohgaki & Kleihues, 2005). The majority of glioma occur in men.

<i>Glioma grade</i>	<i>Histology</i>
I	Benign, slow growing, tumor.
II	Relatively slow growing, cells look slightly abnormal, may spread to nearby tissues.
III	Malignant, cells look abnormal
IV	Extremely malignant, fast growing, cells recruit abnormal vasculature to tumor region, necrotic cells visible. Cells are undifferentiated and anaplastic. Grade IV astrocytoma is known as GBM multiforme.

Table 1. The World Health Organization glioma grading system.

Common molecular alterations in GBM

Gliomas, like many cancers, typically exhibit more than one genetic mutation, referred to as the multi-hit hypothesis (Nordling, 1953). These mutations can involve the deletion of key genes, activating mutations, and copy number alterations leading to overexpression of oncogenes.

The most common genetic alteration in GBM is loss of heterozygosity on chromosome arm 10q, which occurs in 60-90% of GBM patients. Tumors can also arise when a tumor suppressor gene is lost. Loss of gene expression can occur via deletion, methylation, and mutation. One gene in particular that resides on 10q is the *phosphatase and tensin homolog (PTEN)* gene, which is lost in up to 60% of patients with GBM (Wang et al, 1997). Upon ligand binding, growth factor receptors recruit PI3 kinase, which phosphorylates PIP2 creating PIP3, resulting in activation of Akt, a known oncogene

involved in cell proliferation, migration, and angiogenesis. *PTEN* encodes a tumor suppressor protein (Li et al, 1997), which exerts its function by counteracting PI3 Kinase activity, secondarily inhibiting the activation of Akt.

Three major pathways are mutated in GBM. The first is altered expression, activation, or deletion of genes associated with the Tumor Protein 53 (TP53) tumor suppressor gene, which occurs in up to 30% of primary GBM (Ohgaki, 2005; Ohgaki & Kleihues, 2005). TP53, referred to as the “guardian of the genome”, is located on the short arm of chromosome 17. TP53 is responsible for sensing cellular stress and therefore facilitating the transcription of target genes involved in cell cycle arrest, DNA repair, or cellular metabolism. Examples of cellular stress include oxidative stress, DNA damage, osmotic shock, or abnormal oncogene expression. Somatic TP53 mutations are the most common genetic alteration in human cancers, occurring in up to 50% of ovarian cancer, colorectal cancer, and esophageal cancers (Havrilesky et al, 2003; Hollstein et al, 1990; Rodrigues et al, 1990). P53-associated genes are also commonly deregulated in GBM. One of these is the *murine double minute 2 (MDM2)* gene. MDM2, which normally acts as a means to negatively regulate TP53, is commonly amplified in GBM and provides a means to escape TP53-mediated cell cycle control (Wu et al, 1993). Specifically, MDM2 is involved in the ubiquitination and degradation of TP53 protein, and can directly bind to and thereby inhibit TP53-mediating transcription (Burton et al, 2002; Thut et al, 1997). Furthermore, the *CDKN2A* locus, which encodes for p14ARF, is frequently inactivated in GBM either by deletion or other mechanisms. P14ARF, under normal conditions, inhibits MDM2 thereby promoting p53 activity (Moll & Petrenko, 2003; Silva et al, 2003).

The retinoblastoma gene (*RB*) is a tumor suppressor gene involved in cell cycle regulation and is dysfunctional in several human cancers (Murphree & Benedict, 1984). Rb protein is expressed from the *RB* gene located on chromosome 13, and was named retinoblastoma as retinoblastoma cancer would develop if both copies of the gene were

deleted during development. Like TP53, Rb arrests the cell cycle upon sensing cellular stress. An example of cellular stress is when Rb encounters DNA damage. Specifically, Rb binds to E2F and DP protein dimers, thereby inhibiting them (Wu et al, 1995), which results in G1 arrest (Funk et al, 1997). Other Rb-related genes that are dysregulated in GBM include cyclin-dependent kinase (CDK) 4 and CDK6, as well as CDKN2a-P16INK [reviewed in (Bralten & French, 2011)].

Alterations in receptor tyrosine kinase (RTK) pathway signaling constitute another major alteration observed in GBM patients. Specifically, the *epidermal growth factor receptor* (*EGFR*) gene, located on chromosome 7, is aberrantly regulated in up to 50% of GBM cases (Cancer Genome Atlas Research, 2008). Activation of EGFR protein leads to activation of signaling cascades leading to cell proliferation and migration (Carpenter & Cohen, 1990). The EGFR protein is typically membrane bound and becomes activated upon ligand binding, resulting in propagation of downstream signaling cascades. *EGFR* gene deregulation can occur via overexpression or by gene mutation. For example, a mutation in the extracellular domain of the receptor which occurs by deleting exons 2-7, known as EGFRvIII, results in translation of a protein that does not contain the canonical ligand binding domain and is constitutively activated. Interestingly, overexpression of WT receptor usually co-occurs with expression of EGFRvIII (Ekstrand et al, 1991). Overexpression of other RTKs, including the platelet-derived growth factor (PDGF) family are also common in GBM (Hermanson et al, 1992). PDGFs are growth factors that regulate cell proliferation and vascular proliferation. There are four isoforms of PDGF, PDGFA-PDGFD, and two different types of receptors, PDGFRA and B. PDGF ligands are also overexpressed in GBM [reviewed in (Nazarenko et al, 2012)].

Current standard of care

Currently, there is no known cure for GBM. Patients diagnosed with GBM exhibit a median survival of 14 months following diagnosis (Stupp et al, 2009b). Several factors contribute to the deadliness of these tumors. First, GBM are highly heterogeneous tumors, containing several different cell clones and molecular signatures. Secondly, GBM cells are often resistant to most chemotherapy, including TMZ, and as a result typically recur. Finally, due to the location of these tumors, they may invade areas of the brain that are vital to bodily function, making tumor resection exceedingly difficult and compromise neurological morbidity that compromise function.

Upon initial diagnosis of a patient with GBM, a surgeon will attempt to surgically remove as much of the tumor as possible without hurting normal, healthy tissue surrounding the tumor. Sometimes the tumor exists in areas of the brain that make complete resection unlikely. However, partial resection alone provides immense benefit for the patient to alleviate symptoms associated with the tumor, such as relieving pressure created by the tumor. Further, removing a portion or completely removing the tumor allows physicians to properly diagnose the patient, in order to recommend the most suitable next course of action for the patient. During surgery, the brain of the patient is visualized using imaging and monitoring techniques. Some of these imaging techniques include computerized tomography, magnetic resonance imaging, positron emission tomography, and angiography (to map blood vessels). All of these techniques are available to help the surgeon determine the tumor boundaries in order to distinguish the tumor from normal tissue. Following surgical removal, the patient is typically treated with radiotherapy and adjuvant chemotherapy with TMZ (Stupp et al, 2009a).

Radiation is typically administered two to four weeks following surgery. There are three main types of radiotherapy. The most conventional type, called External Beam Radiation Therapy (EBRT), uses a machine that guides radiation from outside of the body.

Brachytherapy involves implanting a radioactive device in or near the tumor. This type of treatment is the most recent advance in radiotherapy. In some instances, patients are offered the opportunity to join clinical trials testing new radiotherapy techniques. Because radiation kills normal, healthy cells in addition to tumor cells, radiation is typically not given repeatedly if the tumor recurs. Radiotherapy combined with surgery has been shown to prolong survival compared to performing surgery alone, however the efficacy of radiotherapy varies between patients (Stupp et al, 2009b).

Chemotherapy treatment has been found to prolong survival in 25% of patients with GBM (Fine et al, 1993). The frontline chemotherapy agent for GBM is called temozolomide (TMZ). The United States Food and Drug Administration approved TMZ in 2005, as it was found to provide a survival benefit while being well tolerated by the patient. TMZ is prodrug that is metabolized by the body to produce the active compound (Figure 1). TMZ exerts its DNA damaging effects by alkylating and methylating DNA at either N-7 or O-6 positions on guanine residues. This resulting methylation triggers the DNA damage response, leading to death of these cells. The ability of cancer cells to bypass TMZ-induced cell death can be partly due to the activity of the O-6-methylguanine-DNA-methyltransferase (MGMT) protein. Specifically, MGMT is able to remove methyl groups added on my TMZ, thus it reverses DNA damage and promotes cell survival (Jacinto & Esteller, 2007). Tumors that lack *MGMT* expression by either epigenetic modification or gene deletion may respond better from treatment with TMZ (Stupp et al, 2009b).

With the advent of sophisticated molecular profiling techniques came the push to provide personalized medicine. A major phenotype observed with GBM is profound vascular proliferation around the tumor site, which provides vital nutrients allowing the tumor to grow and invade nearby tissues. Therefore, the FDA approved the anti-angiogenic drug bevacizumab (Avastin) in 2009 [Avastin Approval History. U.S. Food and Drug Administration]. Furthermore, patients harboring RTK mutations such as the EGFRvIII

mutation showed modest improvements with RTK inhibitors gefitinib or erlotinib (Rich et al, 2004). Current research is focusing on the use of immunotherapy, gene therapy, and more sophisticated targeted therapies for the treatment of GBM. Furthermore, the blood brain barrier (BBB) prevents many agents from reaching the brain, and therefore from providing full therapeutic potential. Therefore, current research is focusing on more effective drug delivery mechanisms to deliver these potent compounds to diseased tissue within the brain. Furthermore, major hurdles involved in treating GBM patients involve overcoming the BBB.

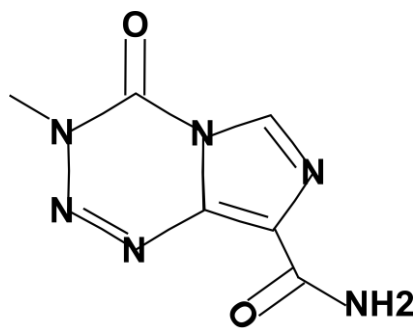


Figure 1. Molecular structure of TMZ.

1.3 Fusion genes

The rearrangement of genetic material inside of a cell, known as genomic instability, can lead to the formation of cancer and other various maladies. Genomic instability is a cellular state that allows the existence genomic alterations such as single nucleotide polymorphisms, gene deletions and amplifications, gene translocations, among other events.

Several factors can lead to genomic instability by damaging DNA, such as radiation, tobacco, or ultraviolet light. Genetic instability can also result from mutating the DNA repair process leading to faulty DNA repair. A consequence of genome instability is the formation, mutation, or overexpression of proto-oncogenes, as well as activating mutations in these

genes. On the other hand, genome instability can lead to the deletion or decrease in expression of tumor suppressor genes.

Another type of genetic event occurs when a particular gene moves to another location on a chromosome, “linking” itself to another gene, forming a hybrid gene. This can also happen when a segment of DNA in between two consecutive genes on a chromosome is deleted. The result of these genetic changes produces a fusion gene. Fusion genes can also contain more than two genes. Fusion genes have been discovered and characterized in a variety of different cancers, ranging from blood leukemias to solid tumors.

In 1973 the first fusion gene was discovered in chronic myeloid leukemia (CML). This fusion contained the central portion of the *breakpoint cluster region (BCR)* gene fused to the second exon of the *abelson murine leukemia viral oncogene homolog 1 (ABL1)* gene (Lifshitz et al, 1988; Nowell & Hungerford, 1960; Rowley, 1973a). Since the initial discovery of this fusion, *BCR-ABL1* has been found to occur in more than 95% of CML patients (Dreazen et al, 1987). This fusion is oncogenic as it encodes a constitutively active ABL1 kinase (Shtivelman et al, 1985b). Since the discovery of *BCR-ABL1*, dozens of fusions have been identified in both hematological and solid cancers, several of which exhibit vast therapeutic benefit when targeted.

Fusion discovery mechanisms

The detection and discovery of fusion genes correlated with the development of more powerful experimental methodologies. Previous use of cytogenetic analysis, such as fluorescent in situ hybridization (FISH) would only detect fusions that contained a significant translocation. Examples of fusions produced by translocations that can be detected by this method are the *EML4-ALK* fusions in lung cancer (Martelli et al, 2009), and *BCR-ABL1* fusions in CML (Shtivelman et al, 1985a). Fusions that cause a particular fusion partner to be overexpressed can be diagnosed via microarray, such as the *TMPRSS2-ERG* fusions in

prostate cancer (Tomlins et al, 2007; Tomlins et al, 2005a). Another example of this is the *MYB-NFIB* fusion in adenoid cystic carcinoma. This fusion contains the majority of the *MYB* gene, and only lacking the 3' untranslated region (UTR) of this gene, connected to the last coding exon of *NFIB*. The *MYB* gene is normally under tight regulation by miR-15a/16 and miR-150, negatively regulating gene expression. However, because this fusion lacks the 3' UTR of *MYB*, this leads to overexpression of the MYB protein (Persson et al, 2009).

Therefore, this is another case where microarray could be used to identify a *MYB-NFIB* positive patient sample. With the advent of more powerful and sophisticated sequencing technologies came the discovery of fusion genes in a diverse array of cancers (Figure 2; Table 2). The first available sequencing technique lead to the published sequence of the *lac* operon, in 1972 (Gilbert & Maxam, 1973). Soon thereafter, a more powerful technology was developed, termed Sanger sequencing (Sanger et al, 1977). Although this technology is nearly 40 years old to date, it is still widely used in research laboratories today. In 1983, the polymerase chain reaction (PCR) was developed by the American biochemist Kary Mullis, which revolutionized biochemistry and molecular biology (Saiki et al, 1985). Applied Biosystems developed the first automated DNA sequencer in 1987, which profoundly decreased experiment effort and overall duration (Wade, Nicholas. 2000).

Fusion name	Discovery year	Discovery method	Reference
<i>BCR-ABL1</i> (CML)	1960	Cytogenetic analysis	(Rowley, 1973a)
<i>IGH-MYC</i>	1972	Cytogenetic analysis	(Manolov & Manolova, 1972)
<i>ESWR1-FLI1</i>	1983	Cytogenetic analysis	(Aurias et al, 1983)

<i>SS18-SSX1</i>	1987	Cytogenetic analysis	(Turc-Carel et al, 1987)
<i>PML-RARA</i>	1990	Cytogenetic analysis	(Larson et al, 1984)
<i>EWSR1-ATF1</i>	1990	Cytogenetic analysis	(Bridge et al, 1990)
<i>ETV6-NTRK3</i>	1998	Cytogenetic analysis	(Knezevich et al, 1998)
<i>PAX8-PPARG</i>	1999	Cytogenetic analysis	(Kroll et al, 2000)
<i>MECT1-MAML2</i>	2003	Cytogenetic analysis	(Tonon et al, 2003)
<i>TMPRSS2-ERG</i>	2005	Microarray technology	(Tomlins et al, 2005b)
<i>TMPRSS2-ETV1</i>	2005	Microarray technology	(Tomlins et al, 2005b)
<i>EML4-ALK</i>	2007	PCR technology followed by Sanger sequencing	(Soda et al, 2007)
<i>KIAA1549-BRAF</i>	2008	PCR technology followed by Sanger sequencing	(Jones et al, 2008)
<i>MYB-NFIB</i>	2009	Cytogenetic analysis	(Persson et al, 2009)
<i>ESRRA-C11orf20</i>	2011	Next-generation	(Salzman et al,

		sequencing	2011)
<i>FGFR3-TACC3</i> (GBM)	2012	Next-generation sequencing	(Singh et al, 2012)
<i>FGFR3-TACC3</i> (BC)	2012	RT-PCR following by Sanger sequencing	(Williams et al, 2013b)
<i>PTPRK-RSPO3</i>	2012	Next-generation sequencing	(Seshagiri et al, 2012)
<i>EIF3E3-RSPO2</i>	2012	Next-generation sequencing	(Seshagiri et al, 2012)
<i>SFPQ-TFE3</i>	2013	Next-generation sequencing	(2013)

Table 2. Fusion genes and their methods of discovery. Taken with permission from Parker, B.C., and Zhang, W. (2013). Fusion genes in solid tumors: an emerging target for cancer diagnosis and treatment. Chinese journal of cancer 32, 594-603.

Several factors hindered DNA sequencing at this time, including the cost, time, and manpower it took to sequence a sample. In 2005 came the development of a high-throughput, low cost sequencing platform, known as next-generation sequencing. This highly sophisticated platform revolutionized genetic sequencing and allowed the production of millions of read sequences concurrently, allowing quicker and easier detection of chromosomal abnormalities across disease samples (Schuster, 2008). Specifically, the detection of fusion genes was completely transformed and was light years easier compared to conventional detection methods.

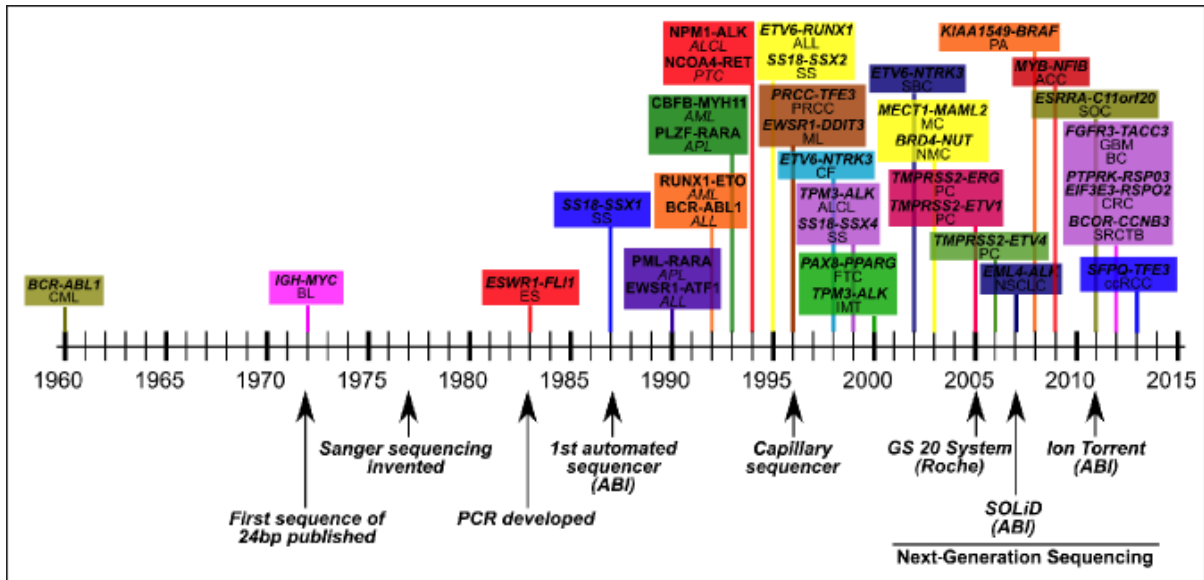


Figure 2. Fusion discovery coincides with sequencing technology. Taken with permission from Parker, B.C., and Zhang, W. (2013). Fusion genes in solid tumors: an emerging target for cancer diagnosis and treatment. Chinese journal of cancer 32, 594-603.

Fusions that do not produce a highly overexpressed protein, or that arise via focal chromosomal rearrangements would go undetected in conventional methodologies. Therefore, the advent of next-generation sequencing allowed researchers to find these hard to find fusions, which helped shed light on the importance of these particular chromosomal aberrations, and how we can utilize them as therapeutic targets in many cancers. Although fusion events were originally associated with hematological malignancies, increasing numbers of fusions have been discovered in solid tumors(Figure 3).

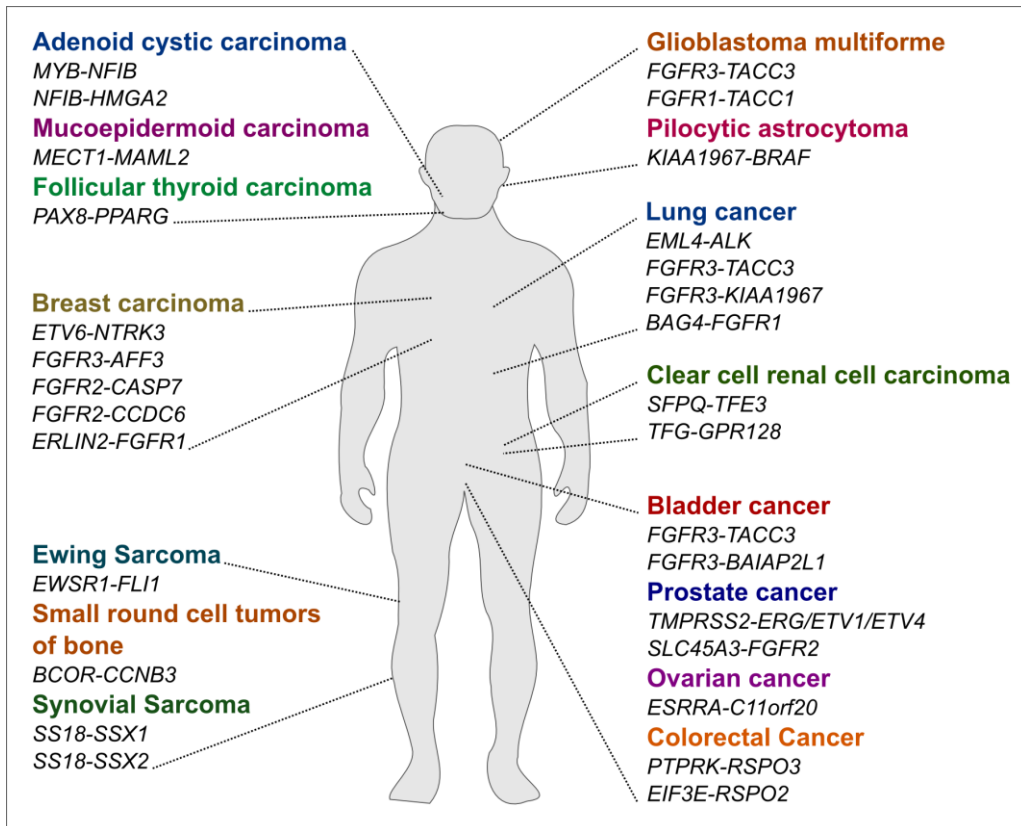


Figure 3. Locations of fusion genes that occur in solid tumors. Used with permission from Parker, B.C., and Zhang, W. (2013). Fusion genes in solid tumors: an emerging target for cancer diagnosis and treatment. Chinese journal of cancer 32, 594-603.

Types of fusion genes

Fusion genes can arise via a variety of mechanisms resulting from chromosomal instability (Figure 4). A fusion forms by deletion when a segment of DNA between two consecutive genes on the same chromosome is deleted, resulting in the union of upstream and downstream genes. An example of a fusion that forms via deletion is the *TMPRSS2-ETS transcription family (ERG, ETV1, and ETV4)* fusion in prostate cancer, which fuses the promoter region of *TMPRSS2* to members of the ETS family transcription family. Expression of the *TMPRSS2* gene is androgen driven. Therefore, formation of this fusion causes the

expression of the *ERG*, *ETV1*, or *ETV4* genes to be regulated in an androgen-dependent manner, leading to their overexpression of these oncogenic signaling proteins (Tomlins et al, 2005a).

Fusion genes can also arise via translocation. Translocation occurs when a segment of DNA moves to another location, or when two chromosome arms switch. An example of a fusion gene that results via translocation is the *BCR-ABL1* fusion. This fusion forms when chromosomes 9 and 22 switch, forming what is called the Philadelphia chromosome (Biesecker et al, 1973). This fusion is oncogenic as it encodes a constitutively active form of the oncogenic ABL kinase (Shtivelman et al, 1985a). And finally, fusion genes can form via inversion, where a segment of DNA is inverted, creating a fusion. An example of a fusion forming via inversion is the *EML4-ALK* fusion in lung cancer, which forms via a small inversion on chromosome arm 2p (Soda et al, 2007).

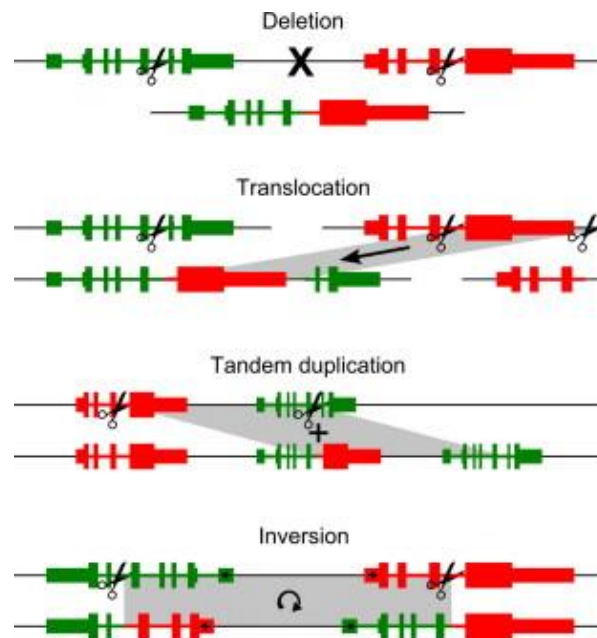


Figure 4. Mechanisms of fusion gene formation. Used with permission from Annala, M.J., Parker, B.C., Zhang, W., and Nykter, M. (2013). Fusion genes and their discovery using high throughput sequencing. *Cancer letters* 340, 192-200.

Therapeutic targeting of fusion genes

Fusion genes are attractive in cancer research because they can serve as prognostic markers, diagnostic tools, and can be used as therapeutic targets. The ability to exploit fusion genes as therapeutic targets was first realized with the *BCR-ABL1* fusion in CML. As mentioned previously, the fusion encodes a constitutively activated *ABL1* RTK. Targeting the fusion by using the *ABL1* inhibitor imatinib substantially prolonged patient survival with patients harboring the *BCR-ABL1* fusion. Similarly, the *PML-RARA* fusion, found in up to 95% of acute promyelocytic leukemia patients, can be targeted by using tretinoin (all-trans retinoic acid). Clinical trials using tretinoin on *PML-RARA* positive patients have revealed impressive therapeutic benefits for these patients (Castaigne et al, 1990; Huang et al, 1988; Larson et al, 1984). The first fusion to be targeted in solid tumors was the *EML4-ALK* fusion, found in 5% of lung cancer patients (Soda et al, 2007). Fusion positive patients were treated with the *ALK* inhibitor crizotinib, which benefited patient survival (Camidge & Doebele, 2012).

Ewing sarcoma is a highly metastatic class of sarcoma and is the second most frequent bone tumor subtype in children. Fusions between the *EWSR1* gene and *ETS* family of transcription factors occur in approximately 90% of these patients, and are produced via translocation between chromosomes 11 and 22. The first detected fusion genes in sarcoma were found in a patient with Ewing sarcoma in 1983 (Aurias et al, 1983; Delattre et al, 1993; Turc-Carel et al, 1983). Evidence suggests that this fusion is correlated with high expression levels of the insulin-like growth factor 1 receptor (*IGF-1R*) (Scotlandi et al, 1996), a transmembrane receptor that promotes cellular transformation and survival (Shelton et al, 2004), and that is upregulated in malignant tissues (LeRoith & Roberts, 2003). Efforts to generate a targeted therapy for *EWSR1-FLI1* positive patients led to the development of molecules that inhibit *IGF-1R*. Although preclinical studies in the laboratory showed potential, when brought to the clinic only a subset of patients with this fusion benefitted from

IGF-1R inhibition (Olmos et al, 2011). Therefore, current efforts are dedicated to the identification of a predictive measure to identify patients who are positive for the *ESWR1-FLI1* fusion who would benefit from IGF-1R targeted therapy.

1.4 Fibroblast Growth Factor Receptor family

The fibroblast growth factor receptor (FGFR) family contains membrane bound receptors that bind to members of the fibroblast growth factor ligand family (over 22 known ligands) (Ornitz & Itoh, 2001). These receptors contain an extracellular ligand-binding domain, which consists of three immunoglobulin-like (Ig-III) domains, a transmembrane domain, and an intracellular domain that possesses tyrosine kinase activity. Upon ligand binding to the extracellular domain, receptors dimerize and the C-terminal domain is then autophosphorylated. This leads to recruitment of adaptor proteins such as grb2, which links active receptors to JAK/STAT3, ERK, and Akt signaling pathways (Dailey et al, 2005). Activation of FGFRs leads to a plethora of functional consequences, including cellular differentiation, proliferation, survival, and migration. There are five members of the FGFR family. FGFRs 1-4 contain the canonical structure as described above. However, FGFR5 lacks a cytoplasmic tyrosine kinase domain (Sleeman et al, 2001).

FGFR expression

FGFR family members are differentially expressed both spatially and temporally, and exhibit preferential ligand binding specificity. Furthermore, each family member can undergo alternative splicing, yielding isoforms that are expressed in specific tissues. For example, the extracellular Ig-III domain of FGFR3 can be alternatively spliced yielding IIIb and IIIc isoforms, which are expressed in epithelium and mesenchyme, respectively (reviewed in (Holzmann et al, 2012)). In adult tissues, FGFR1 is highly expressed in cardiac myocytes, epithelial cells of the heart, pituitary gland, thymus, and cornea, while absent from the

epithelial lining of the stomach. FGFR2 is widely expressed in the brain, ovary, and gastric epithelium. FGFR3 is highly expressed in bone and cartilage, as well as the pancreas. FGFR4 has a more limited distribution, and is observed in the gastrointestinal system (Hughes, 1997).

FGF ligands are also expressed differentially. FGF-1 and FGF-2 are diffusely expressed across adult tissues (Hughes et al, 1993), while other ligands are expressed at different times during development, and vary among tissue types. For example, FGF3, -5, and -4 are mainly expressed during development, but not in adult tissues (Jakobovits et al, 1986; Yoshida et al, 1988).

FGFR and cancer

Several cancers exhibit abnormal FGFR signaling [reviewed in (Dieci et al, 2013)]. For example, FGFR1 mutations have been observed in prostate cancer (Giri et al, 1999) and in GBM (Rand et al, 2005), while FGFR1 amplifications are found in lung and breast cancers (Theillet et al, 1993; Weiss et al, 2010). Moreover, aberrant FGFR2 signaling occurs in breast, gastric, and endometrial cancers (Antoniou et al, 2008; Byron et al, 2012; Jang et al, 2001). FGFR3 is also implicated in cancer. For example, nearly 50% of bladder cancer cases exhibit an activating mutation in the extracellular portion of the FGFR3 (van Rhijn et al, 2002), and the receptor is overexpressed in up to 20% of multiple myeloma patients (Chesi et al, 1997). Furthermore, about 7%-8% of rhabdomyosarcoma patients harbor FGFR4-activating mutations and receptor overexpression (Taylor et al, 2009).

1.5 Transforming Acidic Coiled-Coil Containing Protein 3

The *transforming acidic coiled-coil containing protein 3 (TACC3)* gene is located on chromosome location 4p16.3 and encodes a protein that plays a role in mitotic spindle stabilization during mitosis (Gergely et al, 2000). TACC3 is a member of the TACC family of

proteins, which consists of three proteins that are conserved throughout metazoans. The N-terminal domain of TACC3 contains several phosphorylation sites, while the C-terminal contains a coiled-coil domain. TACC3 is highly expressed in proliferative cell types and regenerative tissues (Hao et al, 2002), and TACC3 knockout mice confer embryonic lethality (Piekorz et al, 2002). TACC3 activity is tightly regulated by Aurora Kinase A phosphorylation, which causes TACC3 to localize to the centrosomal proximal spindle during pro-metaphase (Barros et al, 2005). Other TACC3-interacting molecules include the MT polymerase family XMAP215, which is critical for the growth of centrosomal microtubules (Barros et al, 2005).

TACC3 and cancer

The human TACC1-3 genes are located on chromosomes whose regions show genetic aberrations in many cancers and neurological diseases [reviewed in (Ha et al, 2013a)]. For example, the *TACC1* and *TACC2* genes are commonly amplified in breast cancer, and are associated with worse patient prognosis as well as cancer recurrence (Cheng et al, 2010; Chin et al, 2006). The *TACC3* gene was found to be overexpressed in GBM, and correlated with expression of Aurora Kinase A (Duncan et al, 2010). TACC3 was also found to be upregulated in lymphoma cases, as well as multiple myeloma (Chakraborty et al, 2008; Keats et al, 2003).

CHAPTER 2: Materials and methods

Tumor samples. 40 human glioma samples (20 GBM; 5 anaplastic astrocytoma; 6 anaplastic oligodendroglioma; 9 oligodendroglioma) were acquired from University of Texas MD Anderson Cancer Center's Brain Tumor Center tissue bank. 51 human glioma samples (28 GBM; 23 low-grade glioma) were acquired from the Tumor Tissue Bank of the Tianjin Medical University Cancer Institute and Hospital. Tissues were obtained from surgery and snap frozen. Dr. Kexin Chen's group performed the RT-PCR validation experiments on Tianjin samples.

RNA extraction for transcriptome sequencing. While frozen, each tissue (weighing up to 50 mg) was transferred to a liquid nitrogen-cooled mortar and pestle, crushed into powder, and dissolved in 1 ml TRIZOL reagent (Invitrogen). Chloroform (200 μ l) was added to the sample, which was then vortexed at high speed for 15 seconds and centrifuged at 12,000 g for 15 minutes at 4°C. The aqueous phase was transferred to a fresh 1.5-ml Eppendorf tube, and an equal volume of 70% ethanol was added and the contents mixed by tube inversion. A Qiagen RNeasy mini column (Qiagen) was used to further purify the sample. The column was washed twice with 500 μ l RPE buffer (Qiagen), and RNA was eluted with 50 μ l nuclease-free water. The RNA was quantified using a spectrophotometer. RNA integrity was verified using an Agilent 2100 BioAnalyzer. Poly-A selection was not performed on any of the sample pools.

Sample pooling. Samples were pooled for SOLiD sequencing according to tumor type. GBM samples were divided into four pools of five tumor samples. Anaplastic astrocytoma and anaplastic oligodendroglioma samples were pooled into two separate pools, and the oligodendroglioma samples were further split into two pools. Two pools of commercial

normal brain RNA (Ambion) were also acquired: one pool contained RNA from adult brain, the other from fetal brain.

Library preparation for whole transcriptome sequencing. Libraries for both whole transcriptome and small RNA sequencing were prepared using the small RNA expression kit from Applied Biosystems Inc. (PN 4397682; Life Technologies Corp.), based on the SOLiD System whole transcriptome and small RNA sequencing protocols provided by Applied Biosystems. This was performed by the MDACC sequencing core headed by Dr. Changgong Liu. rRNA was depleted from total RNA using the Invitrogen Ribominus Eukaryotic Kit (PN A1083708; Life Technologies Corp.), and 0.5–1.0 µg rRNA-depleted total RNA was fragmented using RNase III. The fragmented rRNA-depleted total RNA was hybridized and ligated with truncated adaptor mix A from the SOLiD small RNA expression kit. Next, reverse transcription was performed to generate cDNA templates. cDNA was size selected from Novex 6% TBE-urea gel (Invitrogen). The excised gel piece containing DNA 100–200 bp in length was split vertically into four pieces using a razor blade. The size-selected cDNA was further amplified using the supplied primer set containing a six-base-long sequence-specific barcode in approximately 12–15 cycles of PCR. The purified PCR products with barcodes served as a library. Libraries ranged in size from 150 to approximately 250 bp and contained 50- to 150-bp cDNA inserts, quantitated and qualified by Agilent Bioanalyzer 2100.

Library preparation for small RNA sequencing. The sample containing small RNA was hybridized with truncated adaptor mix A provided in the small RNA expression kit. The adaptor mixes were sets of RNA/DNA oligonucleotides with a single-stranded degenerate sequence at one end and a defined sequence required for SOLiD sequencing at the other. Hybridizing and ligating the sample with adaptor mix A sequentially yielded the template for SOLiD sequencing from the 5' end of the small RNA. The small RNA population of 18–40 nt

ligated with adaptor mix A was reverse transcribed to generate cDNAs. To meet the sample quantity requirement for SOLiD sequencing and to append the required terminal sequences to each molecule, the cDNA libraries were amplified using one of the supplied primer sets containing a six-base-long sequence-specific barcode in approximately 12–15 cycles of PCR. The individual library PCR products, containing small RNA of 18–40 nt with barcode(s), were purified and size-selected for 108–130 bp by electrophoresis on 6% polyacrylamide gel.

Template bead preparation. The individual prepared library was quantitated and titrated, before multiplexing, as pooled templates for emulsion PCR; the template molecules were attached to 1 μm beads as described in the Applied Biosystems SOLiD emulsion PCR protocol. After emulsion PCR, the template beads with amplified monoclonal templates were enriched by adaptor P2-affinity binding of polystyrene beads in 60% glycerol gradient by centrifugation. The P2-enriched template beads were further modified by terminal transferase with oligo linker for immobilization to the slide and prepared for deposit on substrate-coated glass slides, as described in the Applied Biosystems protocol.

Sequencing. Sequencing runs were performed on SOLiD version 3.5 for both whole transcriptome RNA sequencing and small RNA sequencing. The library template beads were titrated by workflow analysis to determine the percentage of P2-positive beads in the total template before they were deposited onto slides for sequencing. The number of P2-positive template beads deposited in full chambers of slides with multiplexed five barcoded whole transcriptome libraries and performed in 50 nt of whole transcriptome sequencing, and of P2-positive beads of 10 pooled barcoded libraries on full slide for small RNA sequencing in 35 nt small RNA sequencing, was determined. The average depth of colorspace reads per sample pool was 6.7×10^7 .

Fusion gene discovery. To identify fusion gene candidates, RNA-seq reads from each sample pool were aligned against transcripts from NCBI RefSeq 38. Reads that aligned to known transcripts were assumed to result from normal transcription and were discarded from further analysis. The 5' and 3' ends of unaligned reads were split into two anchors, each 18 nucleotides in length. The paired anchors were aligned against human exon sequences from NCBI RefSeq 38. Anchors with more than three alignments against the exome were discarded as noninformative. Since anchors were short, no mismatches against the reference exon sequences were allowed in anchor alignments. For each read with alignments for both anchors, a list of anchor-based exon-exon junctions was generated by taking a Cartesian product of the two sets of exons to which the anchors aligned. If an anchor pair aligned to an exon-exon junction between two exons from the same gene, all junctions for that anchor pair were discarded, because the read was assumed to originate from some form of unannotated transcription or splicing. We were then left with fusion candidates represented by exon-exon junctions between distinct genes. Once we had the lists of anchor-based junctions for every sample, we combined them and verified the junctions by aligning the full transcriptome-unaligned reads against them.

To reduce the number of false positives, each fusion candidate was required to fulfill the following requirements (Supplemental Figure 1). (a) The fusion candidate must not involve rRNA genes or other highly abundant genes, and must not involve genes located at hypervariable genomic sites. The list of blacklisted gene name patterns included RN18S1, RN28S1, RPPH1, SNORD*, SNORA*, RNY*, RN7SL, RN7SK, RNU*, and HLA-*. (b) Full 50-base reads aligning to the fusion candidate must together cover at least 15 bases on both sides of the fusion junction. (c) The fusion candidate must not be found in Ambion commercial normal brain samples. (d) The fusion candidate's supporting reads must not contain more than an average of 0.7 nt mismatches per read against the reference

transcriptome. (e) The 3' side of the fusion junction must have no perfect alignments against any sequence within 50 kb of the genomic alignment for the 5' side of the fusion junction. The 5' side of the fusion junction must have no perfect alignments against any sequence within 50 kb of the genomic alignment for the 3' side of the fusion junction.

For each fusion fulfilling these requirements, we counted the number of reads in each of the 8 tumor sample pools and calculated a P value using the Pearson χ^2 test to compare goodness-of-fit against a uniform reference distribution. Fusions were then ranked in ascending order by P value, so that fusions whose read distributions deviated most significantly from a uniform distribution were ranked at the top. In total, we identified 17,564 putative fusion junctions supported by one or more RNA-seq reads; filtering yielded a ranked list of 52 fusion candidates.

Small RNA expression analysis based on sRNA-seq. Small RNA sequencing reads were trimmed to a length of 18 colors and aligned against mature microRNA sequences from miRBase version 14 using Bowtie (Langmead et al, 2009). Mature microRNA expression levels were calculated by counting reads that aligned completely within an annotated mature microRNA site in the pre-microRNA sequence. Trimming of reads to 18 colors prior to alignment was necessary because the sRNA-sequence protocol resulted in reads that included a 3' adapter sequence. The trimming step also allowed us to effectively calculate the expression level of each microRNA as the sum of its iso-miR expressions. MicroRNA expression levels were normalized by the total number of mappable reads per sequencing experiment (Moore et al, 2013).

RT-PCR validation of fusion transcripts. To create a mammalian expression vector, cDNA was synthesized using SuperScript III (catalog no. 18080-051; Invitrogen) and random hexamers followed by PCR amplification using Advantage HD polymerase mix (639241;

Clontech) with *FGFR3* primer TCGCCAGTCTCCCGAGC and *TACC3* primer GACAGCGGCTCCGTGGAGG. The fusion PCR products were TOPO cloned (45-0640; Invitrogen). Finally, the MSC enzymes BamHI and XbaI were used to move the fusion genes into pcDNA3.1⁺. All final constructs were sequence verified.

Immunoblot validation of fusion proteins. Total protein was isolated from tumor tissue by subjecting it to lysis buffer (1× RIPA containing 0.1% Halt protease) and phosphatase inhibitor cocktail (Fisher Scientific) and brief sonication (Branson Digital Sonifer Model 450) at 10% amplitude, followed by rotation at 40°C for 30 minutes. Total protein was isolated by centrifugation at 1,214 *g* for 15 minutes, and lysates were stored at –80°C.

Cloning. cDNA (random primed, superscript III) was made from GBM-13, the patient sample with the highest detected fusion level. The complete 3.0-kb fusion transcript was amplified using the forward primer 5'-TCGCCAGTCTCCCGAGC-3' (upstream of the *FGFR3* start codon) and the reverse primer 5'-GACAGCGGCTCCGTGGAGG-3' (downstream of the *TACC3* stop codon) with the Clontech Advantage — LA polymerase kit (catalog no. 639152). The PCR product was cloned into pCR2.1 (catalog no. K4500; Invitrogen). An error-free subclone was created in pcDNA3.1 (by way of a pBluescript II intermediate to pick up required *HindIII-Xba* cloning sites). WT *FGFR3* and *TACC3* constructs were purchased (Origene) and subcloned into the pcDNA3.1 expression vector.

Cell line generation and immunoblotting. All tissue cultures were maintained in DMEM/F12 medium supplemented with 10% FBS in a 37°C humidified incubator containing 5% CO₂. Control cell lines containing pcDNA3.1 expression vector only were obtained as previously described (Wang et al, 2003). The *FGFR3-TACC3* construct sequenced from GBM-13 was inserted into the pcDNA3.1 expression plasmid (Invitrogen) under control of the cytomegalovirus promoter. 6×10^5 SNB19 and U251 cells were transfected with 10

mg *FGFR3-TACC3*, WT *FGFR3*, or WT *TACC3* cDNA with Lipofectamine (Invitrogen) per the manufacturer's instructions. Stably transfected cells were selected for with 0.4 mg/ml G418 (Invitrogen) for two weeks, after which SNB19 clones were selected and amplified. Relative expression of either WT *FGFR3* or the *FGFR3-TACC3* fusion between SNB19 cell clones and the mixed population was measured by immunoblot analysis using a mouse monoclonal antibody probing for *FGFR3* amino acids 25–124 (sc-13121; Santa Cruz Biotechnology Inc.). Downstream analysis after *FGFR3-TACC3* fusion overexpression was performed, probing for β -tubulin (9F3), phosphorylated STAT3 (Tyr705; 3E2), total STAT3 (79D7), phosphorylated p44/42 MAPK (ERK1/2; Thr202/Tyr204), total p44/42 MAPK (ERK1/2), vimentin, lamin B, GAPDH, and total *TACC3* (Santa Cruz Biotechnology Inc.)

miR-99a reporter gene assay. The 3'-UTR of *FGFR3* in the pMirTarget reporter vector was purchased from Origene Technologies Inc. The miR-99a binding site was mutated using QuikChange Lightning Site-Directed Mutagenesis Kit (Agilent Technologies), creating a deleted mutant from 5'-AAUACGGGUA-3' to 5'-AA——UA-3'. To test the ability of miR-99a to target the 3'-UTR of *FGFR3*, WT and mutant constructs were transfected into SNB19 cells concurrently with TK Renilla luciferase reporter vector (Promega) and either control (scrambled) microRNA or miR-99a mimic (Thermo Fisher Scientific). At 48 hours after transfection, cells were assayed for relative luciferase activity using the Dual-Luciferase Reporter Assay System (Promega). Transfections were replicated in 9 independent experiments. In each experiment, relative luciferase activity following miR-99a overexpression was normalized to scrambled controls and converted to a log ratio. An unpaired 1-tailed *t* test was used to determine whether the log ratios were different between WT *FGFR3* UTR and deletion mutant cells.

qRT-PCR validation of successful miR-99a transfection in SNB19 cells. To confirm successful transfection, miR-99a mimic (300516-03), anti-miR-99a (IH-300516-05), and

scrambled (control) microRNA (Thermo Fisher Scientific) were transfected into SNB19 parental cells with 9 biological replicates (transfections) per group. For each of the biological replicates, miR-99a (assay ID 000435; Applied Biosystems) levels were quantified using TaqMan qRT-PCR (microRNA protocol 4364031 revision B; Applied Biosystems) with 3 technical replicates that were averaged and normalized to endogenous U6 (assay ID 001093; Applied Biosystems). A 2-tailed Mann-Whitney *U*test was used to assess whether miR-99a/U6 log ratios differed between groups.

qRT-PCR validation of FGFR3 mRNA level regulation by miR-99a, miR-21, and miR-125b. miR-99a mimic (300516-03), anti-miR-99a (IH-300516-05), miR-21 mimic (C-301023-01), miR-125b mimic (C-300595-03), or scrambled (control) microRNA (Thermo Fisher Scientific) were transfected into SNB19 parental cells with nine biological replicates (transfections) per group. 0.5 µg total RNA from each transfection was reverse transcribed in 20-µl reactions. A ratio of 1 µg total RNA to 0.4 µg random hexamers was maintained, and the mixtures were heated at 70°C for 10 minutes. The tubes were then incubated at room temperature for 10 minutes, and the following components were added: 1× Superscript II RT Buffer (Invitrogen), 10 mM dithiothreitol (Invitrogen), 0.5 mM dNTPs (ISC Bioexpress), 20 U RNase Inhibitor (Ambion), and 200 U Superscript II Reverse Transcriptase (Invitrogen). The reaction was again incubated for 10 minutes at room temperature and then held at 37°C for one hour. The reaction was incubated at 42°C for 1.5 hours and then at 50°C for 30 minutes. Real-time PCR was performed on the Applied Biosystems Prism 7900 using an *FGFR3* assay (Hs00179829_m1; Applied Biosystems) and human cyclophilin A (4326317e) Vic-labeled Pre-Developed Assay Reagent (Applied Biosystems); the 15-µl final reaction volume contained 1× TaqMan Universal PCR Master Mix (Applied Biosystems) and 1× Assay-on-Demand. cDNA (25 ng/well) was amplified with the following cycling conditions: 10 minutes at 95°C, followed by 50 cycles at 95°C for 15 seconds and 60°C for 1

minute. Each qRT-PCR measurement was performed in 3 technical replicates that were averaged and normalized to cyclophilin A. A 2-tailed Mann-Whitney *U* test was used to assess whether FGFR3/cyclophilin A log ratios differed between groups.

Measurement of FGFR3 protein level regulation by miR-99a, miR-21, and miR-125b. To determine whether overexpression of miR-99a mimic or anti-miR, miR-21 mimic, and miR-125b mimic affected FGFR3 protein expression, each respective microRNA was transfected into SNB19 parental cells, and relative FGFR3 expression was measured 48 hours later via immunoblot analysis (Santa Cruz Biotechnology Inc.). Band intensity was quantified and normalized to β -tubulin expression using Image J software (NIH). The experiment was replicated three times.

Generation of FGFR3 WT and fusion constructs containing the 3'-UTR of FGFR3. To generate WT *FGFR3* and *FGFR3-TACC3* fusion constructs containing the 3'-UTR of *FGFR3*, the 3'-UTR of *FGFR3* was amplified by PCR from a *FGFR3* 3'-UTR plasmid (SC215711; Origene Technologies) to introduce the *NheI* cloning sites at both sides (underlined below), using the forward primer 5'-GCTAGCGGGCTCGCGGACGTGAAG-3' and the reverse primer 5'-GCTAGCGGTTAGCAACCAGGTGTC-3'. The PCR product was cloned into pCR2.1 and verified by DNA sequencing. *FGFR3* 3'-UTR was then digested with *NheI* from pCR2.1-*FGFR3* 3'-UTR and subcloned into the *XbaI* sites downstream of pcDNA3.1⁺ WT *FGFR3* and pcDNA3.1⁺*FGFR3-TACC3* vectors. All constructs were verified by DNA sequencing. To determine the ability of miR-99a to regulate expression of *FGFR3* 3'-UTR-containing constructs, miR-99a or scrambled control was transfected and assayed via immunoblot as described previously.

In vitro functional studies. An MTT assay was performed to measure cell viability. Cells were seeded at 650 cells/well in a 96-well plate in quadruplicate and allowed to attach overnight.

Cell viability was measured by incubating cells with 0.5 mg/ml MTT reagent in PBS (Sigma-Aldrich) for two hours. MTT reagent was then aspirated, and cells were subjected to lysis with 100% DMSO. Plates were read at 590 nm using the Tecan SpectraFluor Microplate Reader and Magellan 6 software (Tecan Group Ltd.) at 48, 72, or 96 hours after cell plating. Cell proliferation was measured via BrdU incorporation assay at 7, 11, and 13 hours in triplicate. Briefly, cells were synchronized at G1 by starvation for three days. Fresh medium was then added, and the cells were incubated for 12 hours, followed by pulse labeling with 20 mM BrdU for one hour at the indicated time points. The cells were stained with FITC-conjugated anti-BrdU antibody, incubated with 7-aminoactinomycin-D (7-AAD), and quantified via flow cytometry. To determine whether *FGFR3-TACC3* promotes colony formation in soft agar, empty vector, *FGFR3-TACC3*, WT *FGFR3*, and WT *TACC3* SNB19 or U251 stable cells were cultured in DMEM/F12 medium with 10% FBS in the log phase. The soft agar was prepared by mixing 1.5% sterile low melting point agarose in PBS with fresh medium at a 1:2 dilution. Soft agar (1 ml of 0.5%) was added to each well of a 6-well plate and kept at room temperature for 15 minutes. Cells were then harvested and suspended in 0.375% soft agar at 1,000 cells/ml. This cell suspension (1 ml) was added on top of the prepared base agar layer. The plates were incubated for two weeks and fed two times per week. Colonies were counted under a microscope, and relative colony size was measured using AxioVision 3.1 software. Scratch migration, or wound healing, assays were performed using the 33mm culture-inserts purchased from Ibidi. Within each chamber, 70 μ l of a 500,000 cells/ml suspension was added. Cells were incubated at 4°C until they reached confluence, at which point the chambers were removed, leaving behind a 500 μ m-wide border that was absent of cells, referred to as the “scratch”. Cells were imaged at 5X every several hours until the scratch closed.

Gene expression microarray analysis on fusion clones. *FGFR3-TACC3* fusion– or WT *FGFR3*–transfected SNB19 mixtures or clones were hybridized onto dual-channel Agilent Whole Human Genome 4 × 44K v1 microarrays. RNA from parental SNB19 cells was hybridized onto the reference channel. Microarray slides were imaged, and background adjusted probe intensities were calculated using Agilent Feature Extraction Software version 9.1.3.1. Probe sequences were aligned against RefSeq 38 transcript sequences, and the probes were arranged into probesets based on the genes they aligned against. Background-adjusted probe intensities were quantile normalized and summarized using the robust multiarray analysis (RMA) algorithm (Irizarry et al, 2003). Differential gene expression was calculated by comparing against the reference channel. Pathway analysis was performed using Ingenuity Pathway Analysis (IPA; version 11904312). Microarray was performed by Limei Hu. Microarray files have been deposited in GEO (accession no. GSE42401).

Intracranial xenograft implantation and tissue preparation. Male athymic mice (*nu/nu*) were implanted in the brain with EV, *FGFR3-TACC3* fusion, or WT *FGFR3* cells. Briefly, mice were anesthetized with 0.25 ml of a cocktail of 10 mg/ml ketamine and 1 mg/ml xylazine, and cells were implanted using cranial guide screws as previously described (Lal et al, 2000). A Hamilton syringe and microinfusion syringe pump (0.5 ml/min; Harvard Apparatus) were used to implant 1×10^6 cells into the brain of ten mice simultaneously, as described previously (Nakamizo et al, 2005). Upon detection of an external tumor or obvious declining health, mice were sacrificed by intracardiac perfusion of PBS and 4% paraformaldehyde. Brains were extracted and fixed in 10% formalin for 24 hours, embedded in paraffin, and sectioned into 5-mm slices.

Immunohistochemical staining. For immunohistochemical staining, Dako Envision+System–horseradish peroxidase and diaminobenzidine (DAB) were used (Dako). Briefly, after antigen retrieval for 10 minutes in 0.1 M citrate buffer (pH 6.0) or 1 mM EDTA (pH 8.0) and

subsequent incubation in peroxidase block solution for 5 minutes at room temperature, the sections were incubated overnight at 4°C with rabbit anti-human FGFR3 (1:600; Abcam), pSTAT3 (1:200, Tyr705 D3A7; Cell Signaling Technology), and pERK (1:200, T202/Y204; Cell Signaling Technology). The sections were incubated in peroxidase-labeled polymer for 30 minutes at room temperature, and the signals were revealed with DAB⁺ substrate–chromogen solution. For negative controls, primary antibodies were replaced with PBS.

Localization. Fusion localization was performed by using the Q Proteome Cell Compartment Kit (Qiagen) according to manufacturer’s instructions. Briefly, cells were lysed and differential centrifugation performed using various buffer systems to isolate the cytosol, membrane, nuclear, and cytoskeletal fractions. Cell fractions were then run on an immunoblot. Immunofluorescence was performed and imaged via confocal microscopy.

bFGF and EGF stimulation. To determine whether the *FGFR3-TACC3* fusion exhibits ligand dependence or independent firing, EV, *FGFR3-TACC3* fusion, and WT *FGFR3* cells were seeded in 6-well plates and incubated with 50 ng/ml bFGF or EGF ligand for 30 minutes at 37°C. Cells were then harvested and subjected to immunoblot, probing for FGFR3, phosphorylated ERK, total ERK, and actin (Santa Cruz Biotechnology Inc.).

Drug treatment studies. For studies measuring cell viability after U0126, WP1066, PD172074, or TMZ drug treatments, EV, WT *FGFR3*, and *FGFR3-TACC3* fusion cells were plated at 100,000 cells/well in a 96-well plate. 12 hours after plating time, “0” was read to ensure cells were plated in equal numbers. At this time, drugs were added in increasing concentrations, with DMSO only as control. Plates were assayed 48 hours later, and values were normalized to DMSO controls. Cells were also seeded in 6-well plates and incubated with each inhibitor for one hour. These cells were assayed via immunoblot to determine the

potency of each drug concentration. A subG1 assay was performed on cell lysates by use of propidium bromide and analyzed via flow cytometry.

Statistics. Unless otherwise indicated, data are represented as mean \pm SEM. Statistical analyses were performed using Fisher exact test, Mann-Whitney *U* test, 2-way ANOVA, 1- or 2-tailed Student's *t* test, and log-rank test, as indicated. Activation *z* scores were calculated as defined in the Ingenuity white paper "Ingenuity Downstream Effects Analysis in IPA." Mice that died of causes other than cancer were considered censored. A *P* value of 0.05 or less was considered significant.

Study approval. Glioma tissue samples from the Brain Tumor Center tissue bank of the University of Texas MD Anderson Cancer Center were collected under an institutional review board–approved protocol. Glioma tissue samples from the Tumor Tissue Bank of the Tianjin Medical University Cancer Institute and Hospital were collected with approval from the institutional review board. All subjects provided informed consent of their participation in the study. Implantation of cells into the brains of male athymic mice were performed according to institution-approved protocols.

Note: A portion of these materials and methods were obtained with permission from a published study in *The Journal of Clinical Investigation* (Parker et al, 2013a).

CHAPTER 3: Results

3.1 The FGFR3-TACC3 fusion gene occurs in 8.3% of GBM patients

Rationale. Recurrent fusion genes have been reported in a variety of cancers, beginning with the initial discovery of the *BCR-ABL1* fusion in chronic myeloid leukemia (Rowley, 1973b). The development of next-generation sequencing provided an enormous opportunity to discover fusion genes that were unable to be detected using conventional methodologies. Furthermore, as of 2009 a recurrent fusion gene in glioma had yet to be reported. Therefore, by using next-generation deep sequencing technology, we hypothesized a recurrent fusion gene could be identified in glioma.

Results. To determine whether recurrent fusion genes existed in glioma, whole transcriptome sequencing was performed on glioma tissues of varying grades. RNA from tissues were grouped together by grade, forming RNA pools. Adult normal brain was used as a control. RNA-seq reads that spanned exon-exon junctions connecting two discrete genes were prioritized according to specific criteria (Figure 5).

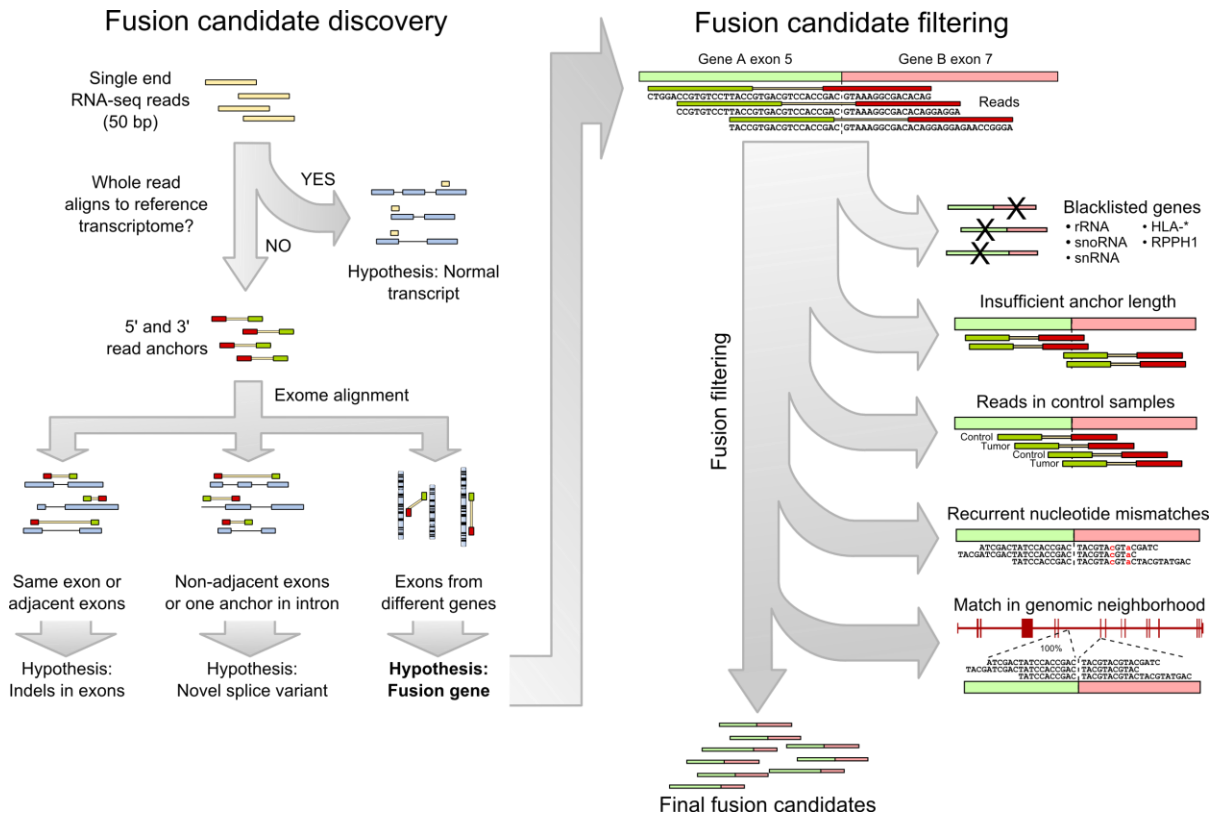


Figure 5. Fusion filtering algorithm. A fusion-filtering algorithm produced a ranked list of fusion candidates while filtering out false positives. Bioinformatics analysis was performed by Matti Annala. Used with permission from Parker, B.C., Annala, M.J., Cogdell, D.E., Granberg, K.J., Sun, Y., Ji, P., Li, X., Gumin, J., Zheng, H., Hu, L., *et al.* (2013a). The tumorigenic *FGFR3-TACC3* gene fusion escapes miR-99a regulation in glioblastoma. *The Journal of clinical investigation* 123, 855-865.

The fusion with the highest recurrence rate that satisfied all criteria contained the Fibroblast Growth Factor Receptor 3 (*FGFR3*) gene linked to the Transforming Coiled-Coil containing protein 3 (*TACC3*) gene. This fusion, *FGFR3-TACC3*, contained four unique reads, with 16 reads in total (Figure 6). Interestingly, this fusion was found in a GBM pool, and was not found in any low grade or normal brain pools. To determine whether fusion

Figure 6. Breakdown of fusion candidate discovery (A) yielded the top fusion candidate, *FGFR3-TACC3*, based upon 16 reads, four of which were unique (B). Adapted and used with permission from Parker, B.C., Annala, M.J., Cogdell, D.E., Granberg, K.J., Sun, Y., Ji, P., Li, X., Gumin, J., Zheng, H., Hu, L., *et al.* (2013a). The tumorigenic *FGFR3-TACC3* gene fusion escapes miR-99a regulation in glioblastoma. *The Journal of clinical investigation* 123, 855-865.

The fusion was then validated using RT-PCR. Specifically, primers were designed that flanked the fusion breakpoint, one on the *FGFR3* side and another on the *TACC3* side of the breakpoint. PCR was then performed, and the resulting PCR product sequenced. If the sequenced result contained both *FGFR3* and *TACC3* genes, then the patient was considered positive for the *FGFR3-TACC3* fusion. The fusion was found in 4/48 GBM patient samples (8.3%), but not in any lower grade or normal brain samples. Three separate fusion breakpoints were observed, which contained variable breakpoints in the *TACC3* gene. However, all fusion variants contained the same breakpoint on the *FGFR3* side, exon 18. One variant connected exon 19 of *FGFR3*, but because this exon does not have a splicing donor site, it instead fused exon 18 of *FGFR3*. The first and most common variant connected to *TACC3* exon 11 (Figure 7 A,B), while a longer variant was found which connected to *TACC3* exon 4.

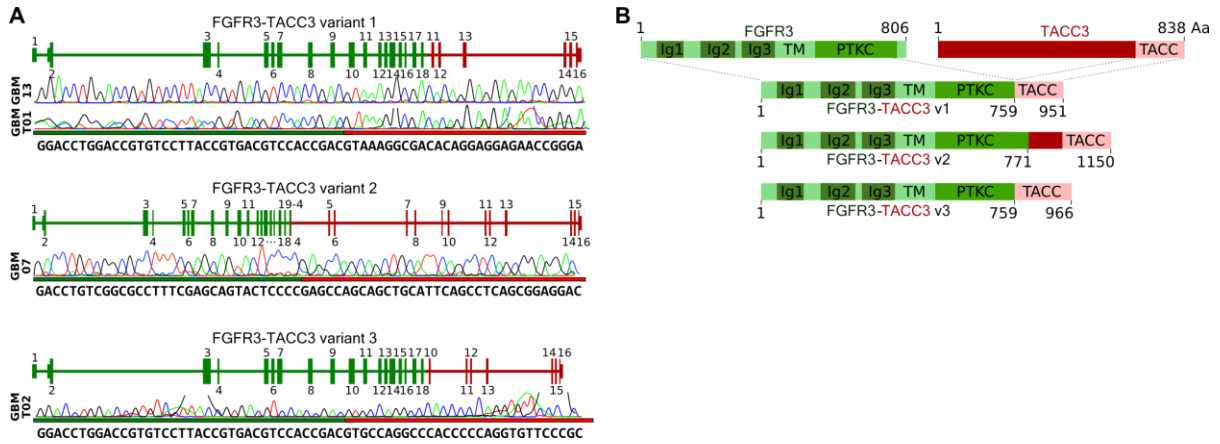


Figure 7. *FGFR3-TACC3* fusion validation. Exon transcript structures and electropherograms from *FGFR3-TACC3* positive patient samples (A) along with protein domain map (B). RT-PCR was performed by David Cogdell. Adapted and used with permission from Parker, B.C., Annala, M.J., Cogdell, D.E., Granberg, K.J., Sun, Y., Ji, P., Li, X., Gumin, J., Zheng, H., Hu, L., *et al.* (2013a). The tumorigenic *FGFR3-TACC3* gene fusion escapes miR-99a regulation in glioblastoma. *The Journal of clinical investigation* 123, 855-865.

The nucleotide sequence of the fusion lead us to believe it translated into an in-frame fusion protein. To test this, SNB19 and U251 cell lines were transfected with the coding region of both fusion variants, the shorter variant with breakpoint at *TACC3* exon 11, known as “Fusion S,” or longer variant with breakpoint at *TACC3* exon 4, known as “Fusion L.” Whole cell lysates were then run on a gel and immunoblotted using an antibody that recognized the N-terminal of *FGFR3*. This particular epitope was chosen because the fusion lacked the C-terminal of *FGFR3*; therefore an antibody that recognized the C-terminal of *FGFR3* would therefore not recognize the fusion (Figure 8A). The fusion was easily recognized by a shift upwards on the blot, indicative of the extra *TACC3* domain. We then tested the ability of a C-terminal *TACC3* antibody to recognize the fusion. Unfortunately, the fusion was unable to be recognized by this antibody, indicating the epitope of this particular

antibody must be upstream of *TACC3* exon 4 (Figure 8B). To determine whether fusion positive patients could be visualized via immunoblot, we then ran RT-PCR fusion positive patient samples alongside cell line controls, containing either stable cell lines (indicated by asterisk) or transiently transfected cell lines. Fusion positive patients were easily observed via immunoblot, and showed strong band patterns (Figure 8C). Interestingly, a single lower molecular weight band was observed in patient GBM-19, although this particular patient was fusion negative. Efforts to determine whether this patient contained an *FGFR3* splice variant were inconclusive. Immunohistochemistry is a useful tool for diagnostic purposes in the clinic. Fusion positive patients showed strong *FGFR3* staining, indicating the presence of the fusion in these samples. Interestingly, all fusion negative patient samples, as well as normal brain samples, showed very low to no levels of *FGFR3* WT (Figure 8D).

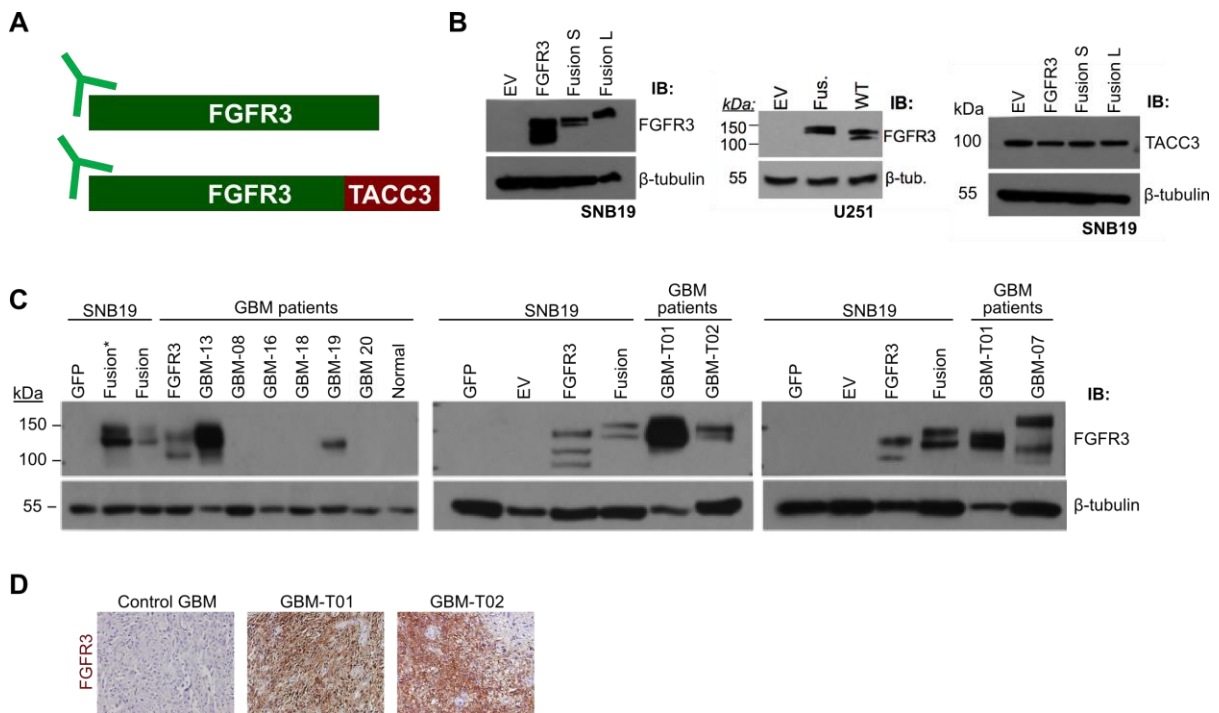


Figure 8. The *FGFR3-TACC3* fusion forms an in frame fusion protein. Schematic of antibody binding to the N terminal of *FGFR3* WT or *FGFR3-TACC3* protein (A). Ability of N-terminal domain to distinguish fusion from *FGFR3* WT stable cell lines. A C-terminal *TACC3* antibody does not recognize the fusion (B). Fusion-positive patient samples at RNA level

show strong fusion protein expression in both immunoblot (C) and immunohistochemical analysis (C). Adapted and used with permission from Parker, B.C., Annala, M.J., Cogdell, D.E., Granberg, K.J., Sun, Y., Ji, P., Li, X., Gumin, J., Zheng, H., Hu, L., *et al.* (2013a). The tumorigenic FGFR3-TACC3 gene fusion escapes miR-99a regulation in glioblastoma. *The Journal of clinical investigation* 123, 855-865.

3.2 The FGFR3-TACC3 fusion escapes microRNA regulation

Rationale. Both immunoblotting and immunohistochemical analyses revealed that fusion-negative patient samples, as well as normal brain, showed little to no FGFR3 WT expression. However, fusion positive patients showed high fusion protein expression. Upon inspection of the fusion transcript sequence, we observed that the 3' UTR of FGFR3 was lost upon formation of the fusion (Figure 9A). Therefore, we hypothesized that the fusion was expressed because it lacked the 3' UTR of FGFR3, enabling it to be undetected by microRNA that normally keep FGFR3 WT levels in check.

Results. To determine whether FGFR3 WT expression was decreased in GBM and brain tissues because of microRNA regulation, the highest expressed microRNA in GBM and normal brain were determined. Specifically, small RNA sequencing was performed on the same pools of glioma and normal brain tissues that were originally used to discover the fusion. A ranked list of microRNA was produced (Figure 9B). The Targetscan.org software was then utilized to determine whether any of these highly expressed microRNA was predicted to target FGFR3 WT. Interestingly, miR-99a, one of the highest expressed microRNA in both GBM and normal brain, was predicted to target FGFR3 WT (Figure 9A).

To determine whether miR-99a indeed targeted FGFR3 WT in GBM, the 3' UTR of FGFR3 was cloned in an expression vector alongside the luciferase gene. Site-directed mutagenesis was performed to delete the miR-99a binding site (Figure 9A). Then, the WT

FGFR3 3' UTR (WT) or miR-99a binding site deleted UTR (Mut.) was transfected into SNB19 cells. These cells were then transfected with miR-99a, and luciferase assay conducted. Luciferase activity was significantly decreased upon transfection of WT UTR, while the Mut. UTR showed no change in luciferase activity (Figure 9C). These results indicate that indeed miR-99a targets the 3' UTR of WT FGFR3 in GBM.

To determine whether these results translated to FGFR3 expression levels, control, miR-99a mimic, or miR-99a anti-miR was transfected into SNB19 cell lines (Figure 9D), which resulted in an inverse correlation between FGFR3 WT RNA expression and miR-99a (Figure 9E). This same pattern was also observed at the protein level (Figure 9F,G).

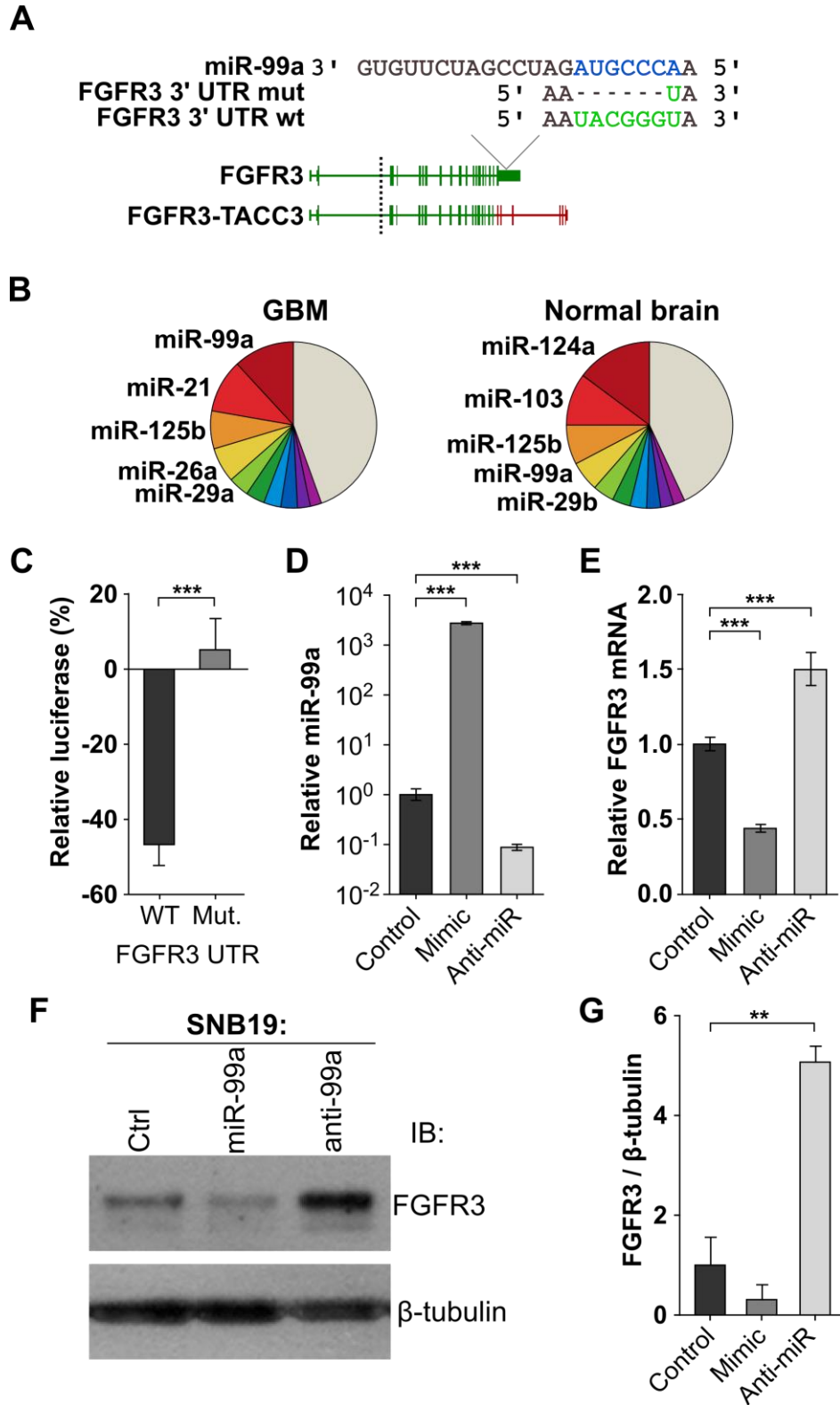


Figure 9. MiR-99a is overexpressed and targets FGFR3 in GBM. Schematic showing the location of the miR-99a binding site in the 3'-UTR of WT *FGFR3* and its loss in the *FGFR3*-

TACC3 fusion transcript and construct with the binding site deleted (mutant) (A). Pie chart illustrating high miR-99a expression in both GBM and normal brain. Expression values were calculated based on pooled small RNA sequencing (B). Luciferase assay of WT *FGFR3* 3'-UTR versus mutant after miR-99a overexpression (C). qRT-PCR of miR-99a in parental SNB19 cells after transfection of control, miR-99a mimic, or anti-miR-99a (D). qRT-PCR (E), immunoblotting (F), and densitometry (G) of FGFR3 in parental SNB19 cells after transfection of control, miR-99a mimic, or anti-miR. Error bars denote SEM (K). ** $P < 0.01$, *** $P < 0.001$, Mann-Whitney U test. Used with permission from Parker, B.C., Annala, M.J., Cogdell, D.E., Granberg, K.J., Sun, Y., Ji, P., Li, X., Gumin, J., Zheng, H., Hu, L., *et al.* (2013a). The tumorigenic FGFR3-TACC3 gene fusion escapes miR-99a regulation in glioblastoma. *The Journal of clinical investigation* 123, 855-865.

To further validate that the fusion is able to be highly expressed because it lacks the 3' UTR of FGFR3, the 3' UTR was cloned back onto the coding region of both FGFR3 WT and the fusion (Figure 10A,B). Cells were transfected in duplicate with EV, WT FGFR3 lacking the 3' UTR, or the WT FGFR3 coding region with 3' UTR attached. Then, cells were transfected with either control miRNA, or miR-99a. Whole cell lysates were taken and samples immunoblotted with antibodies recognizing FGFR3 and β -tubulin as a loading control. FGFR3 protein expression decreased only when the 3' UTR of FGFR3 was transfected along with miR-99a (Figure 10C). This experiment was repeated, but with the coding region of the fusion, or fusion with 3' UTR of FGFR3 added. The same result was obtained (Figure 10D).

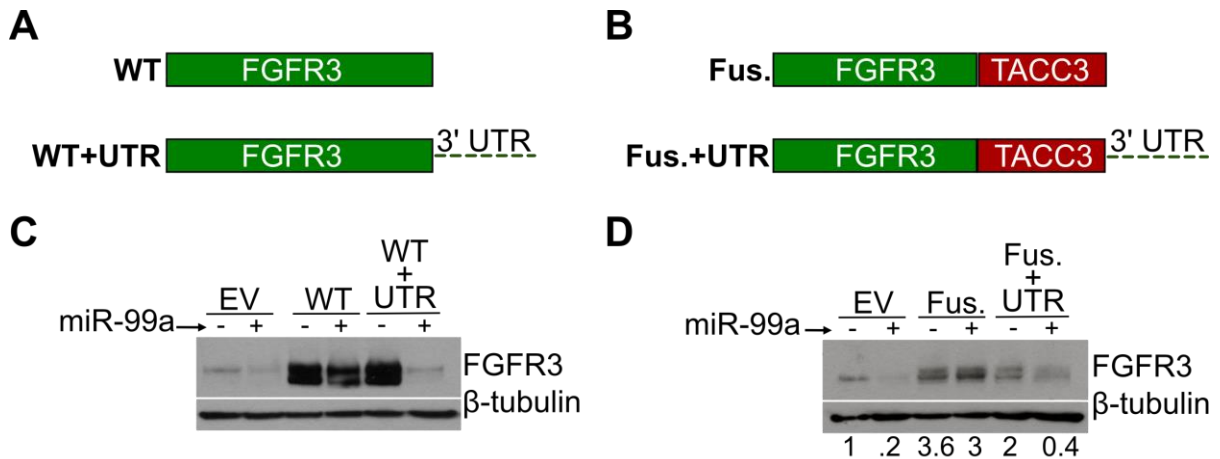


Figure 10. The *FGFR3-TACC3* fusion escapes miR-99a regulation. Schematic of WT *FGFR3* (A) and *FGFR3-TACC3* fusion (B) cDNA, with or without *FGFR3* 3'-UTR attached. Immunoblot of EV, WT *FGFR3*, and WT *FGFR3* plus *FGFR3* 3'-UTR after transfection with miR-99a (C). Immunoblot of EV, *FGFR3-TACC3* fusion, or *FGFR3-TACC3* fusion plus *FGFR3* 3'-UTR after miR-99a transfection (D). Relative densitometry (below) was normalized to β -tubulin. Xia Li contributed to cloning experiments. Used with permission from Parker, B.C., Annala, M.J., Cogdell, D.E., Granberg, K.J., Sun, Y., Ji, P., Li, X., Gumin, J., Zheng, H., Hu, L., *et al.* (2013a). The tumorigenic *FGFR3-TACC3* gene fusion escapes miR-99a regulation in glioblastoma. *The Journal of clinical investigation* 123, 855-865.

TargetScan.org analysis revealed that out of the highest expressed microRNA, miR-99a was the only predicted to target *FGFR3* WT. To validate this result, SNB19 cells were transfected with control microRNA, miR-99a, miR-21, and miR-125b. As expected, only miR-99a was able to deplete *FGFR3* mRNA and protein expression (Fig. 11A-C).

Bladder cancer is known to exhibit activating *FGFR3* mutations and amplification. To determine whether there was an inverse correlation between *FGFR3* expression and miR-99a levels, GBM cell lines U373, U87, and SNB19 were run on an electrophoresis gel

alongside bladder cancer cell lines SW780, RT112, and RT4. All bladder cancer cell lines exhibited increased *FGFR3* WT expression compared to all three GBM cell lines (Figure 11D). To determine whether these tissues contained lower miR-99a, qRT-PCR was performed measuring relative levels of miR-99a in these samples. As expected, GBM cell lines exhibited higher miR-99a expression compared to all three bladder cancer lines (Figure 11E). To determine the ability of the fusion to target miR-99a, relative levels of miR-99a were examined in fusion positive and negative patient samples, and no difference was observed (Figure 11F). These results conclusively show that the fusion is able to bypass miR-99a regulation via loss of the 3' UTR of *FGFR3*. These results also shed light on why levels of *FGFR3* WT are so low in normal brain and GBM, as they're under negative regulation of the highly expressed miR-99a in these tissues.

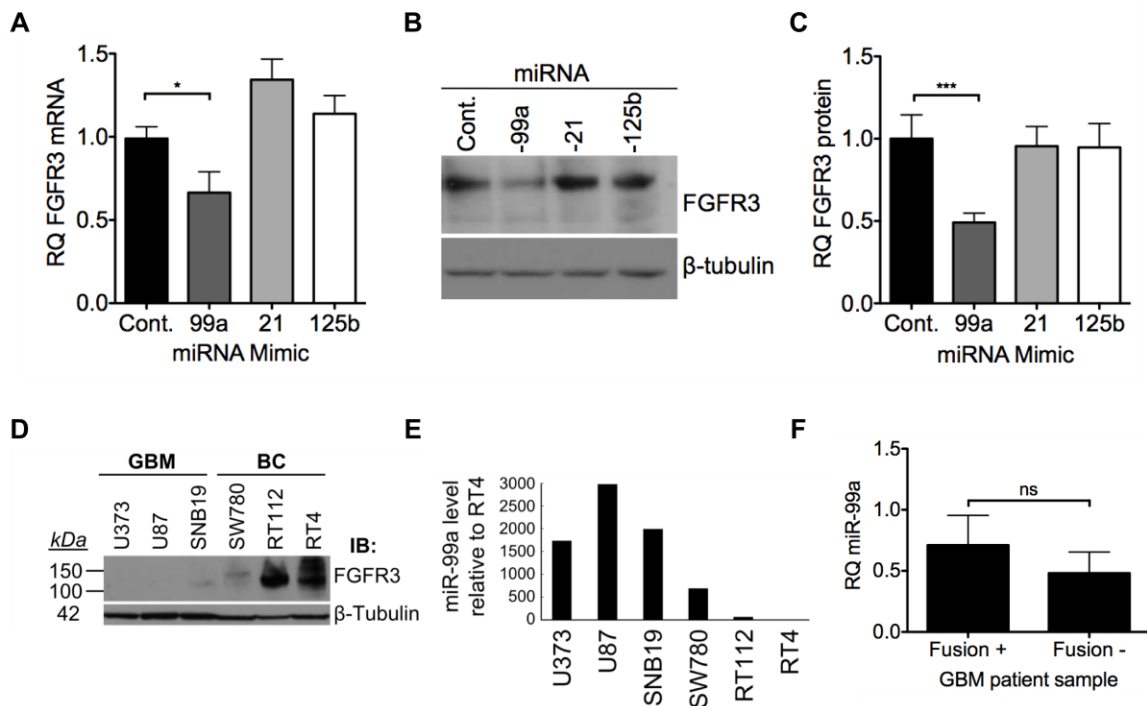


Figure 11. Of the highest expressed miRNA in GBM, only miR-99a suppresses *FGFR3* expression. Upon miR-99a, -21, or -125b transfection, relative *FGFR3* mRNA or protein levels were measured by qRT-PCR (A), immunoblotting (B), and densitometry (C),

respectively. Error bars, s.e.m. P- values calculated using Student's t-test. *P<0.05; ***P<0.001. FGFR3 immunoblot and miR-99a qRT-PCR for three GBM and three bladder cancer (BC) cell lines (D). FGFR3 protein level is inversely correlated with miR-99a (E). There is no difference in miR-99a expression in fusion positive or negative patient samples. Adapted from and used with permission from Parker, B.C., Annala, M.J., Cogdell, D.E., Granberg, K.J., Sun, Y., Ji, P., Li, X., Gumin, J., Zheng, H., Hu, L., *et al.* (2013a). The tumorigenic FGFR3-TACC3 gene fusion escapes miR-99a regulation in glioblastoma. *The Journal of clinical investigation* 123, 855-865.

3.3 The FGFR3-TACC3 fusion activates ERK and STAT3 signaling

Rationale. The FGFR3 is a RTK that activates the canonical Erk, Stat3, and Akt signaling pathways (Dailey et al, 2005). Because the fusion contained the majority of FGFR3, we hypothesized that the fusion would activate Erk, Akt, and Stat3 signaling. The ability of the fusion to activate these pathways was then determined.

Results. To determine whether the fusion activated canonical FGFR3 WT signaling pathways, EV, Fusion, and FGFR3 WT cells were run on an immunoblot and immunoblotted for FGFR3, STAT3, ERK, and AKT. GAPDH was used as a loading control. The fusion was found to primarily activate ERK and STAT3 signaling, with little to no effect on AKT signaling, on either transiently transfected (Figure 12A) or stable cell lines (Figure 12B). For functional studies, stable clones were selected from fusion and FGFR3 WT mixture cells. Once again, fusion-expressing cells showed high ERK activation compared to EV control (Figure 12C).

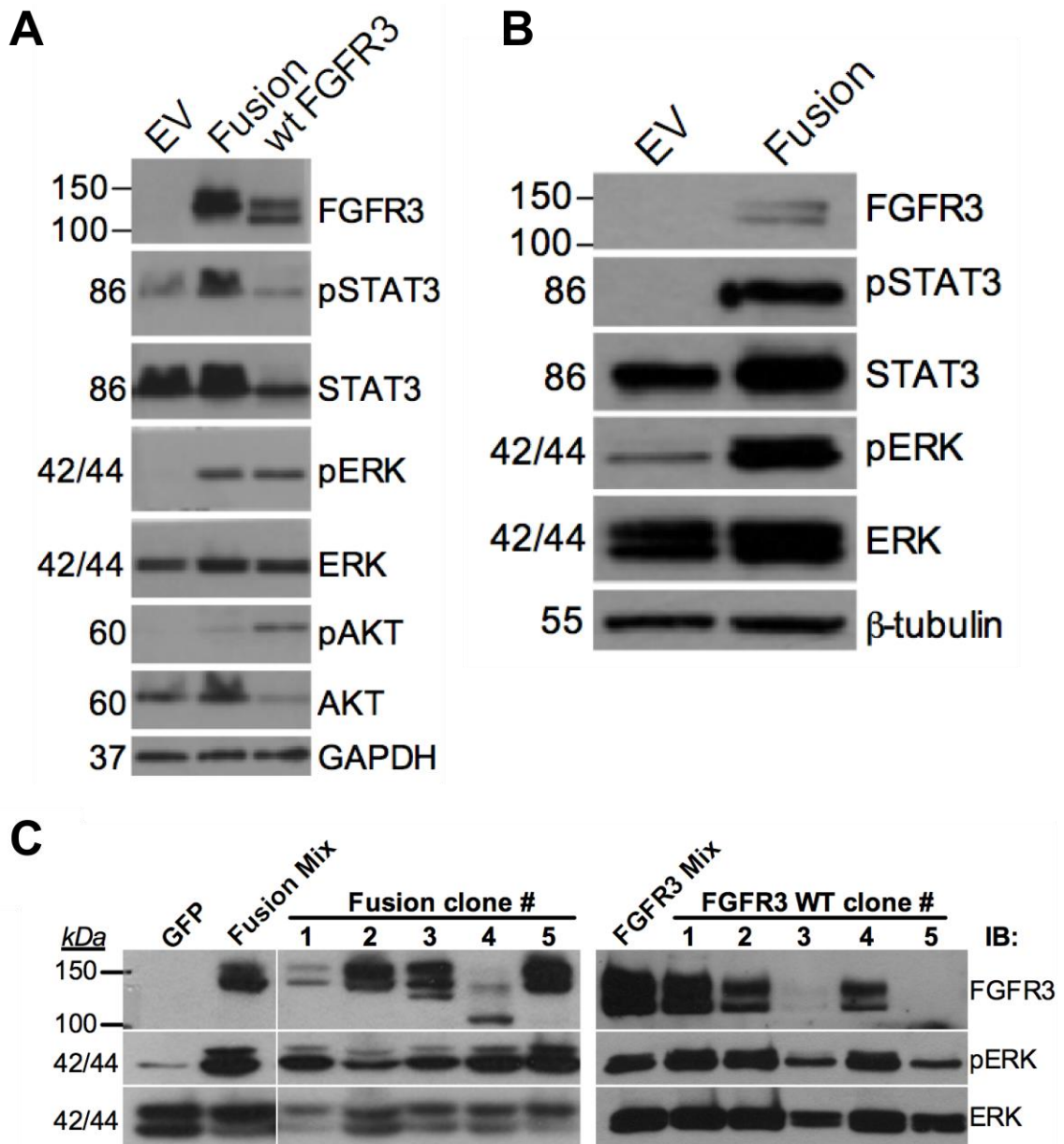


Figure 12. The *FGFR3-TACC3* fusion promotes ERK and STAT3 activity. Downstream analysis of transient (A) and stable (B) fusion cell lines indicates the major downstream molecules activated are STAT3 and ERK. AKT is not significantly activated by the presence of the fusion. SNB19 cell lines were transfected with either fusion or WT cDNA constructs and stable clones selected. Subsequent protein expression is can be visualized via immunoblot (C). Adapted from and used with permission from Parker, B.C., Annala, M.J., Cogdell, D.E., Granberg, K.J., Sun, Y., Ji, P., Li, X., Gumin, J., Zheng, H., Hu, L., *et al.*

(2013a). The tumorigenic FGFR3-TACC3 gene fusion escapes miR-99a regulation in glioblastoma. *The Journal of clinical investigation* 123, 855-865.

3.4 The FGFR3-TACC3 fusion exhibits an oncogenic phenotype *in vitro*

Rationale. The abilities of a cell to divide uncontrollably and invade nearby tissues are hallmarks of cancer, described in the groundbreaking review by Weinberg and Hanahan (Hanahan & Weinberg, 2011). Therefore, because the fusion was discovered in high-grade glioma tissue, we hypothesized that the fusion was oncogenic *in vitro*. The ability of the fusion to promote an oncogenic phenotype *in vitro* was also determined.

Results. To determine whether the fusion exhibited an oncogenic phenotype *in vitro*, EV, FGFR3 WT, and fusion cell lines were subject to an MTT cell viability assay over the course of three days. Briefly, cells were seeded in replicates of 6 in a 96-well plate and assayed every 24 hours. Over the course of the experiment, there were more numerous fusion cells indicated by a higher absorbance measurement, concluding that fusion cells proliferate at a faster rate than either EV or FGFR3 WT cells (Figure 13A). To validate these results, a BrdU incorporation assay was performed and once again, fusion cells proliferated at a faster rate (Figure 13B).

Usually, non-cancerous cells will only divide when attached to a hard surface. Therefore, a measure of oncogenic activity *in vitro* is to perform a soft-agar colony formation assay, where cells are seeded in soft agar and measured for colony number and size over a period of time. The larger and more numerous colonies that form in soft agar is indicative of an oncogenic phenotype. Briefly, EV, TACC3 WT, FGFR3 WT, and fusion cells were seeded in triplicate in a 6 well plate, on top of soft agar and incubated at for several days. As expected, fusion cells showed larger and more numerous colonies, indicating they are oncogenic *in vitro* (Figure 13C).

To gain greater insight into the gene sets activated by the fusion, a microarray experiment was performed on extracted RNA from EV and fusion expressing SNB19 cells followed by Ingenuity Pathway Analysis (IPA). Interestingly, fusion cells exhibited expression of genes that correlate with tumorigenesis, cancer, and neoplasia – further confirming that the fusion activates specific gene pathways promoting an oncogenic phenotype.

To determine whether fusion cells migrated at a faster rate, EV, FGFR3 mixture, Fusion mixture, and Fusion clone 5 (Figure 12C) cells were subject to a scratch migration assay. Briefly, cells were seeded and allowed to grow to confluency. A scratch was then made, and photographed over the course of 24 hours. Both Fusion mixture and Fusion clone 5 cells migrated at a faster rate compared to either EV or FGFR3 WT cells (Figure 13F). Interestingly, fusion clone 5 cells also showed the highest degree of GTP-Rac activation (Figure 13E). Therefore, these results collectively indicate the fusion is highly oncogenic *in vitro*, by exhibiting increased cell proliferation, anchorage-independent cell growth, expression of gene sets correlated with neoplasia and cancer, and cell migration.

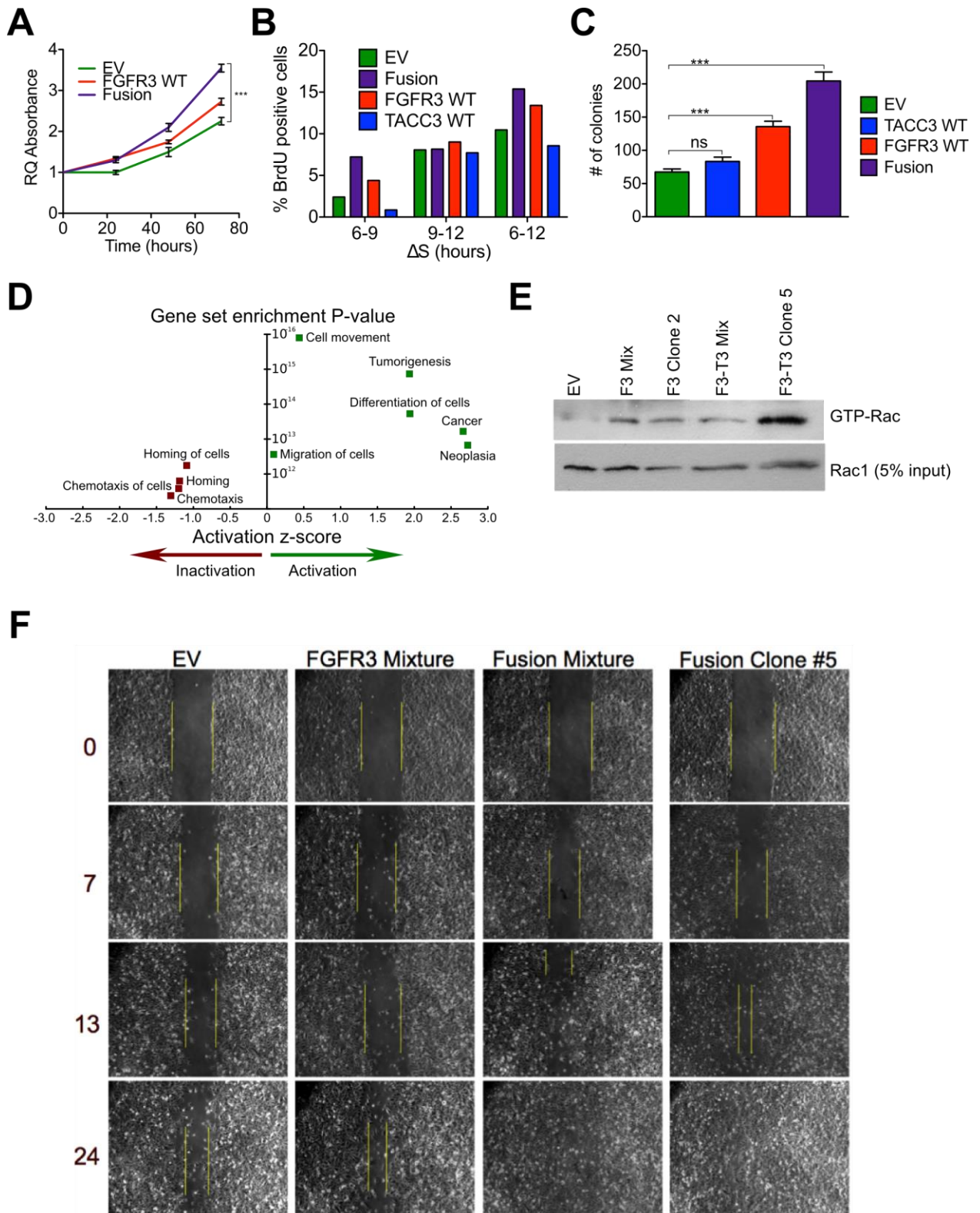


Figure 13. The *FGFR3-TACC3* fusion is oncogenic *in vitro*. The fusion promoted cell proliferation in both MTT (B), and BrdU incorporation assays (B), as well as anchorage-

independent cell growth (C). The fusion exhibited expression of gene sets correlated with tumorigenesis (D), and promoted cell migration (E,F). ***P<0.001. Adapted from and used with permission (A-D) from Parker, B.C., Annala, M.J., Cogdell, D.E., Granberg, K.J., Sun, Y., Ji, P., Li, X., Gumin, J., Zheng, H., Hu, L., *et al.* (2013a). The tumorigenic FGFR3-TACC3 gene fusion escapes miR-99a regulation in glioblastoma. *The Journal of clinical investigation* 123, 855-865. Dr. Ping Ji assisted with BrdU incorporation assay.

3.5 The FGFR3-TACC3 fusion is oncogenic *in vivo*

Rationale. Mouse models are valuable tools to measure the causal effect of potential oncogenes before targeted therapy can be introduced in clinical trials. Mouse models can also be used to test the efficacy and toxicity of potential drug therapeutics.

The fusion exhibited an oncogenic phenotype *in vitro*, including cell proliferation, anchorage-independent cell growth, and migration. Further, upon analysis of genes expressed by the fusion indicated gene sets whose expression correlated with oncogenic gene networks. Because of this, we hypothesized that the fusion was oncogenic *in vivo*. Therefore, the oncogenic potential of the fusion *in vivo* was examined.

Results. To determine whether the fusion was oncogenic *in vivo*, an orthotopic intracranial xenograft mouse model was utilized. Briefly, EV, Fusion mixture (FT^{mix}), fusion Clone 5 (FT^{high}), FGFR3 WT mixture, or FGFR3 Clone 2 (FGFR3 high) were implanted into the brains of immune incompetent mice (Figure 14A). Mice are then sacrificed upon physical inspection of tumor or hydrocephalus. Fusion-implanted mice died at a significantly faster rate compared to either EV or FGFR3 WT mice (Figure 14B, C). Interestingly, FGFR3 WT-implanted mice died at a similar rate to EV (Figure 14B, D). These results suggest that the fusion, indeed, is oncogenic *in vivo*, and that the loss of the C-terminal FGFR3, or the presence of both FGFR3 and TACC3 are required to confer this oncogenic phenotype.

To observe if the same signaling pathways activated by the fusion *in vitro* were also activated *in vivo*, brains of tumor burdened mice were sectioned and stained for FGFR3, phosphor-STAT3, and phosphor-ERK. Agreeing with *in vitro* results, mice that had fusion-positive tumors had increased activation of both signaling pathways (Figure 14E).

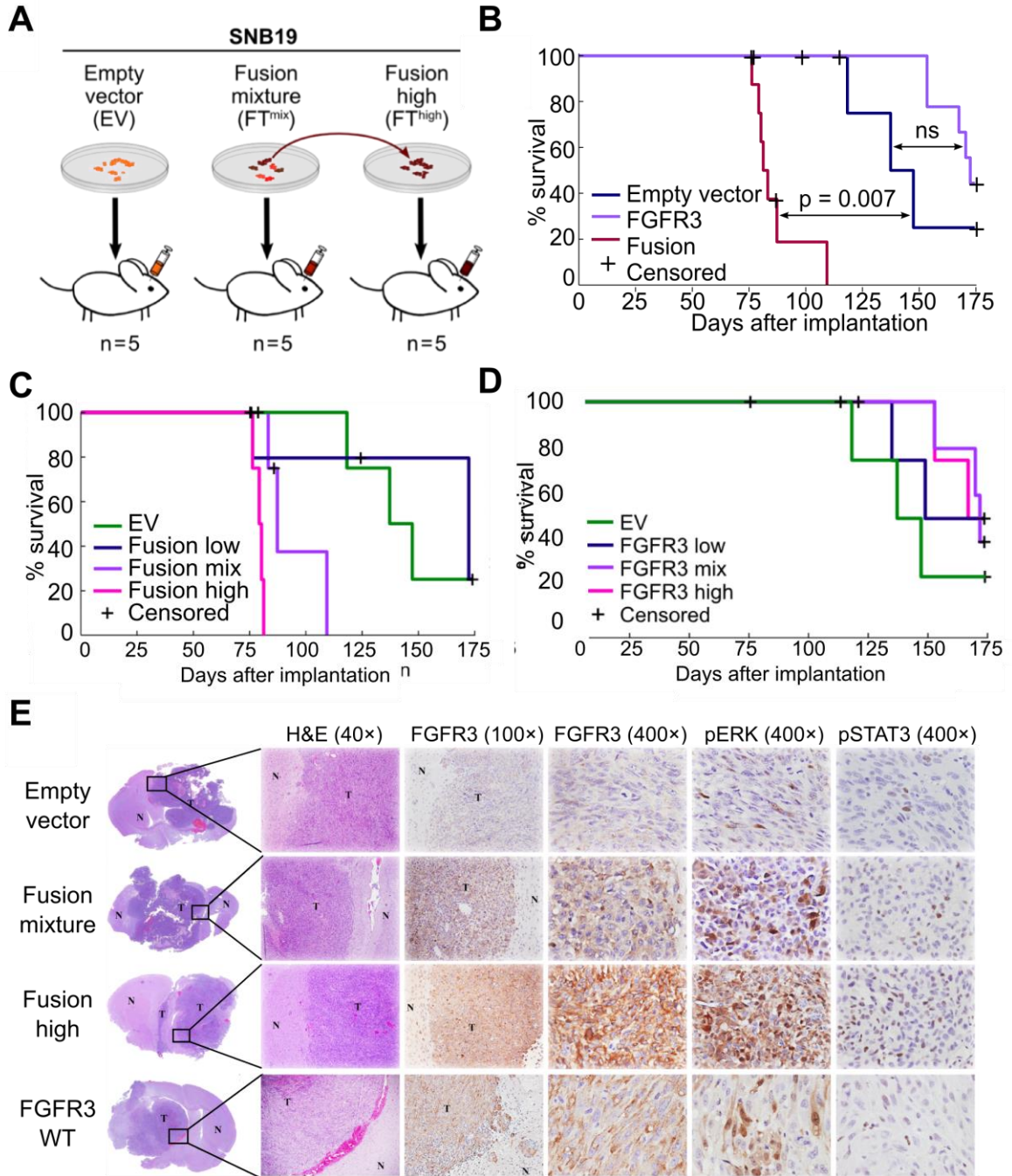


Figure 14. The *FGFR3-TACC3* fusion is tumorigenic *in vivo*. SNB19 stabling expressing cell lines were transplanted into the brains of immunocompromised mice (A). Survival curves of cell lines were analyzed (B-D). Immunohistochemistry confirmed the fusion activates ERK and STAT3 signaling (E). Adapted and used with permission from Parker, B.C., Annala,

M.J., Cogdell, D.E., Granberg, K.J., Sun, Y., Ji, P., Li, X., Gumin, J., Zheng, H., Hu, L., *et al.* (2013a). The tumorigenic FGFR3-TACC3 gene fusion escapes miR-99a regulation in glioblastoma. *The Journal of clinical investigation* 123, 855-865. Joy Gumin, M.S. from Dr. Frederick Lang's and Dr. Yan Sun contributed to these experiments.

3.6 The FGFR3-TACC3 fusion localizes to the nucleus

Rationale. WT FGFR3 protein has been described to localize to the cell membrane, while WT TACC3 is found in the cytoplasm and nucleus (Garriga-Canut & Orkin, 2004). FGFR3 has been found to localize to the nucleus in some cancers, whereas activating FGFR3 mutations in skeletal disorders show limited cell-surface FGFR3 (Bonaventure et al, 2007; Zammit et al, 2001). We hypothesized that the fusion would localize to the membrane and nucleus, as it contained portions of both FGFR3 and TACC3.

Results. To determine where in the cell the fusion localized, a cell fractionation experiment was performed on EV, fusion, FGFR3 WT, truncated FGFR3, and TACC3 overexpressing cell lines. The truncated FGFR3 construct contains the portion of WT FGFR3 contained within the fusion (Figure 15A). Briefly, cellular compartments were separated via differential centrifugation and various buffer systems, as described in the Q Proteome Cell Fractionation kit (see Materials and Methods). The various cell fractions were then run on a polyacrylamide gel and subject to immunoblotting. Using the FGFR3 antibody the location of FGFR3 containing proteins was determined. The fusion was found to primarily localize to the membrane, nuclear, and cytoskeletal fraction, while WT FGFR3 and tFGFR3 were predominantly located in the membrane fraction. WT TACC3 protein was predominantly found in the cytoplasm fraction. GAPDH was used as a cytoskeletal control, lamin as nuclear control, and vimentin as cytoskeletal control. EV^{cyto} was run on the nuclear and cytoskeletal fraction blots as a transfer control (Figure 15B).

To further validate these results, immunofluorescence was performed on FGFR3 WT and fusion-overexpressing SNB19 cells. Once again we can see that the fusion primarily localizes to the membrane and nuclear regions, while WT FGFR3 is on the membrane (Figure 15C).

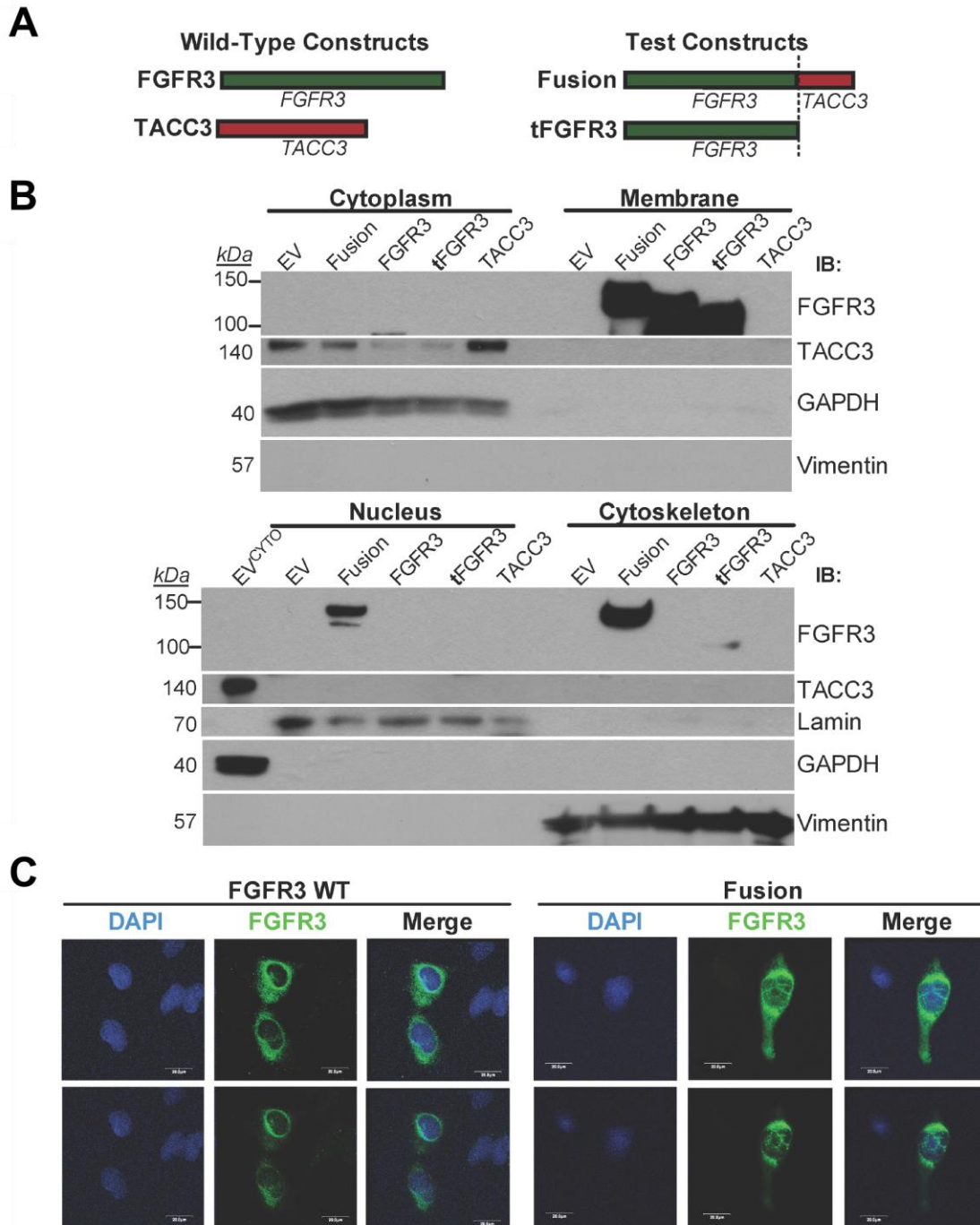


Figure 15. The fusion is localized to the membrane, nucleus, and cytoskeleton.

A schematic of either wt FGFR3 or TACC3 constructs, or test constructs are shown (A) that are used in cell fractionation experiments (B) as well as immunofluorescence (C).

3.7 The FGFR3-TACC3 fusion is activated by bFGF ligand

Rationale. Several (>20) FGFR activating ligands have been described, which differentially activate the four FGFR isoforms. Basic FGF “bFGF” has been shown to activate most receptor isoforms (Dvorak & Hampl, 2005), so we sought to determine whether bFGF could therefore also activate the fusion. Because EGFR amplification is common in GBM, we also sought to determine whether the fusion would respond to EGF treatment, or whether it exhibited constitutive activation. ERK activity was used as a measure of receptor activation following treatment with either bFGF or EGF on serum starved cells.

Results. To determine if the fusion responds to bFGF treatment, EV, FGFR3, and fusion expressing cells were serum starved and then treated with 50ng/mL bFGF for 5, 30, and 60 minutes. ERK activity was measured as a readout for receptor activity. Interestingly, fusion cells exhibited ERK activity in the absence of serum, indicating the fusion is constitutively activated. However, ERK activity increased upon treatment with bFGF, indicating that the fusion, indeed, responds to ligand treatment (Figure 16A).

EGFR is a commonly amplified RTK in GBM. EGFR is activated by EGF ligand binding, resulting in Grb2 recruitment and subsequent ERK activation. To determine whether EGF activated the fusion, EV, FGFR3 WT, and fusion cells were serum starved and then incubated with 50ng/mL EGF for varying amounts of time. Fusion cells did not exhibit differential ERK activation in the presence of EGF, indicating that they do not respond to EGF ligand. Also, because EGFR expression is the same in these cell lines (Figure 16B),

these results suggest that the fusion recruits ERK away from EGFR signaling pathways, and become “addicted” to fusion-induced ERK signaling.

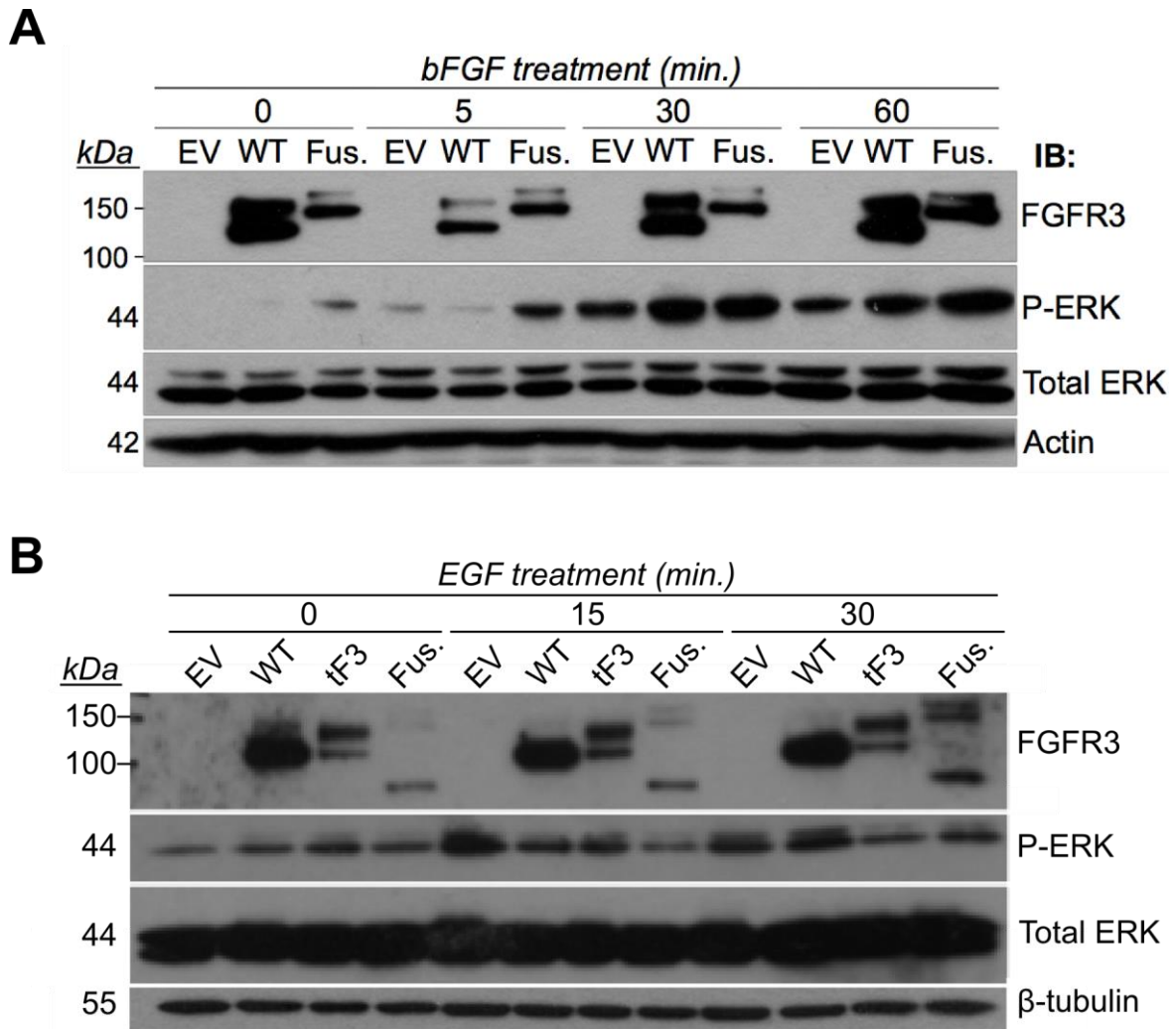


Figure 16. The *FGFR3-TACC3* fusion is activated by bFGF ligand treatment (A), but not EGF treatment (B). Panel (A) is used with permission from Parker, B.C., Annala, M.J., Cogdell, D.E., Granberg, K.J., Sun, Y., Ji, P., Li, X., Gumin, J., Zheng, H., Hu, L., *et al.* (2013a). The tumorigenic *FGFR3-TACC3* gene fusion escapes miR-99a regulation in glioblastoma. *The Journal of clinical investigation* 123, 855-865.

3.9 The FGFR3-TACC3 fusion is chemoresistant

Rationale. TMZ is the frontline chemotherapy agent for the treatment of GBM, and was approved by the United States Food and Drug Administration in 2005. Chemotherapy treatment has been found to prolong survival in 25% of patients with GBM (Fine et al, 1993). One of the biggest hurdles with TMZ treatment is that tumors can become resistant to it, and can recur with a vengeance. Therefore, we sought to determine whether the fusion promoted chemoresistance, and if this was due to expression of genes associated with cell survival and DNA repair.

Results. To determine whether fusion positive cells were targetable by TMZ, a sub G1 assay was performed on EV, fusion, or FGFR3 WT cells upon treatment with 50 μ M TMZ. Fusion expressing cells exhibited less sub g1 activity or apoptotic activity, suggesting a chemoresistant phenotype (Figure 18A). To validate this finding, EV, fusion, FGFR3 WT, and tFGFR3 expressing cells were treated with increasing doses of TMZ over the course of 7 days. Fusion expressing cells exhibited greater cell survival compared to all other cell types (Figure 18B).

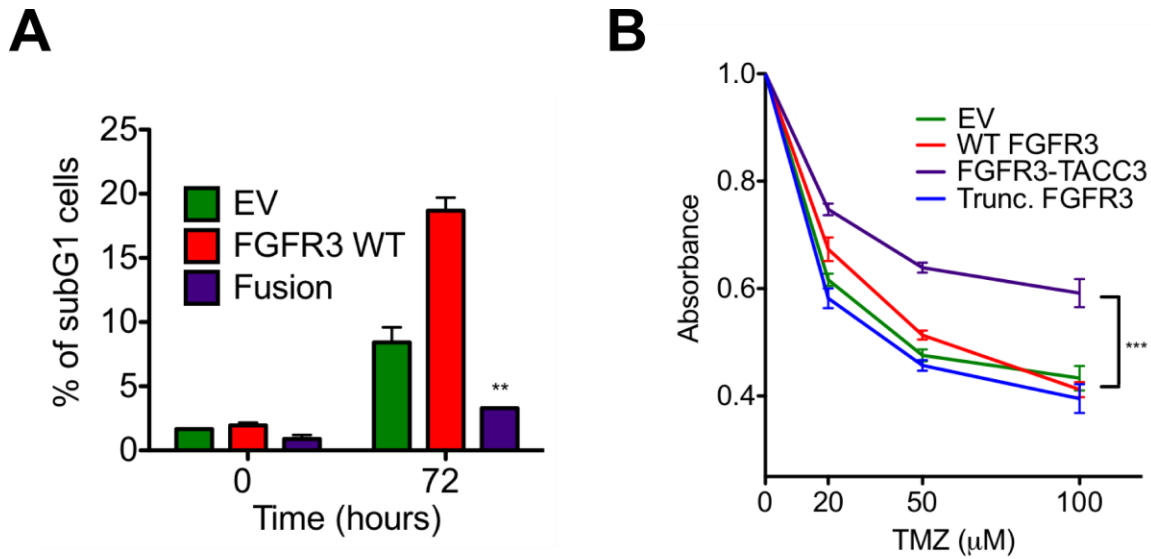


Figure 18. The *FGFR3-TACC3* fusion is chemoresistant. Result determined by sub G1 apoptosis assay (A) and MTT cell viability assay (B).

3.1.1 The *FGFR3-TACC3* fusion is sensitive to targeted therapy

Rationale. The fusion was found to primarily activate ERK and STAT3 signaling, but was found to be chemoresistant. Therefore, we hypothesized that fusion was more sensitive to ERK, STAT3, and FGFR3 inhibitors. If these inhibitors were found to be potent on fusion cells, then it would provide insight into whether these drugs may be useful for fusion-positive patients future clinical trials.

Results. To determine whether the fusion was sensitive to ERK inhibition, EV, FGFR3 WT, and fusion cells were treated with increasing doses of the MEK inhibitor U0126. MEK is directly upstream of ERK, and directly activates it via phosphorylation. Therefore, U0126 is thought to directly impact ERK activity. Briefly, cells were seeded in a 96 well plate and incubated with varying doses of U0126 (with DMSO only as control) for 48 hours. Cells were then assayed via MTT and normalized to DMSO controls. Fusion positive cells were more sensitive to MEK inhibitor U0126 at all doses (Figure 20A). As a control for U0126 potency,

a six-well plate was also utilized and whole cell lysates obtained after treatment with varying doses of inhibitor. Lysates were run on a polyacrylamide gel and immunoblotted with FGFR3, phosphor-ERK, total ERK, and β -tubulin as loading control. A ponceau stain was also performed to ensure correct loading. As expected, fusion cells showed increased ERK activity upon treatment with DMSO control. The potency of U0126 is observed by a steady decrease in ERK activity with increasing drug concentration (Figure 20B).

STAT3 activity was also increased in fusion expressing cells. To determine whether fusion cells were more sensitive to STAT3 inhibitor WP1066, cells were treated with increasing doses over the course of 48 hours. Fusion expressing cells were found to be more sensitive to STAT3 inhibition (Figure 20C). The WP1066 doses chosen were effective at inhibiting STAT3 activity (Figure 20D).

Because levels of FGFR3 WT are low in normal brain and GBM, treatment with an FGFR3 specific inhibitor seems like a successful therapeutic option for fusion positive patients. Therefore, we sought to determine whether fusion positive cells were more sensitive to FGFR3 inhibition. As expected, fusion positive cells were indeed more sensitive to FGFR3 inhibition (Figure 20E,F).

These results suggest that fusion positive patients may benefit from treatment with ERK, STAT3, and FGFR3 inhibition, either alone or in combination. Whether these drugs are potent *in vivo* alone or in combination remains to be elucidated.

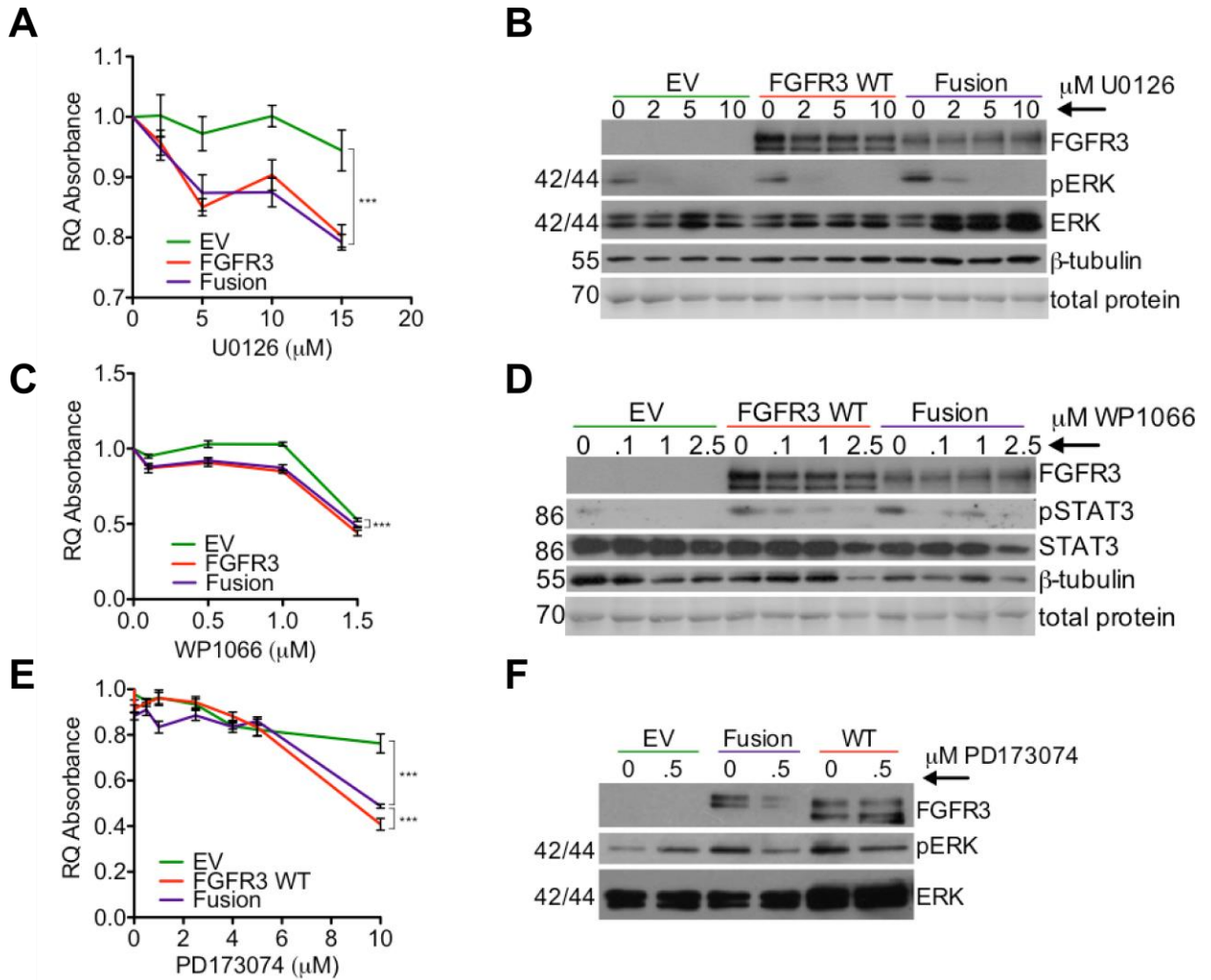


Figure 20. The *FGFR3-TACC3* fusion is more sensitive to targeted therapy. MTT cell viability assays were performed using MEK (A), STAT3 (C), and FGFR (E) inhibitors. Immunoblotting confirmed the potency of each drug used (B,D,F). *** $P < 0.001$. Adapted and used with permission from Parker, B.C., Annala, M.J., Cogdell, D.E., Granberg, K.J., Sun, Y., Ji, P., Li, X., Gumin, J., Zheng, H., Hu, L., *et al.* (2013a). The tumorigenic *FGFR3-TACC3* gene fusion escapes miR-99a regulation in glioblastoma. *The Journal of clinical investigation* 123, 855-865.

CHAPTER 4. Summary

Fusion genes are extremely valuable discoveries in cancer, as they can serve both as prognostic markers and also as drug targets in a clinical setting. The first discovered and characterized fusions were found in leukemia, which proved to be successful therapeutic targets. With the advent of more powerful sequencing technologies, more fusion genes were unveiled in solid tumors. Using next-generation deep sequencing techniques, we discovered the recurrent fusion, *FGFR3-TACC3* in GBM. We found the fusion to be extremely oncogenic both *in vitro* and *in vivo*. The fusion was found to escape microRNA regulation by loss of the 3' UTR on *FGFR3* upon formation of the fusion. Although resistant to treatment with TMZ, the fusion was sensitive to targeted therapy using FGFR, STAT3, and ERK inhibitors.

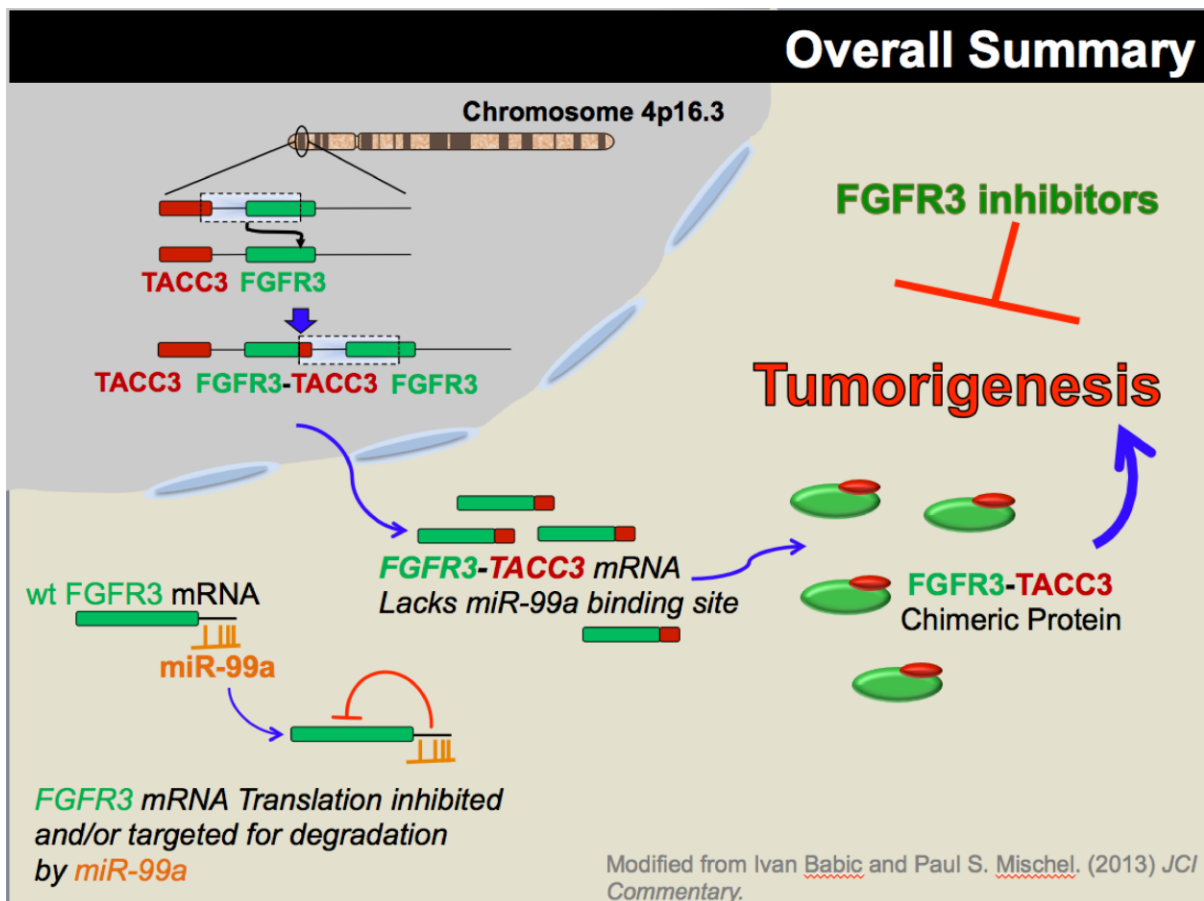


Figure 22. Summary.

CHAPTER 5: Discussion

5.1 The *FGFR3-TACC3* fusion gene knows no cancer boundaries.

Upon the initial discovery of the *FGFR3-TACC3* fusion in GBM, the fusion was discovered in other cancers, including bladder, oral, and lung cancers (Williams et al, 2013a; Wu et al, 2013b). Also, the fusion has recently been found in low-grade glioma by the TCGA working group. It's extremely interesting how one particular fusion can form in very different cancer types. The specific FGFR3 isoforms are also reflected in these fusions, as FGFR3 IIIb isoform is typically expressed in epithelial tissues (i.e. bladder), while the IIIc isoform is expressed in mesenchymal tissues (i.e. brain, lung) (Holzmann et al, 2012).

Interestingly, other FGFR family fusions were also reported in a diverse array of solid cancers (Figure 22). Two of three *FGFR1* fusions contained *FGFR1* as the 3' partner gene, while all *FGFR3* and most of *FGFR2* fusions contained FGFR as the 5' partner gene. Interestingly, All *FGFR2* and *FGFR3* fusions (with one isolated FGFR2 case, *SLC45A3-FGFR2*) contained the same exonic breakpoint – exon 18 or exon 19 in either *FGFR2* or *FGFR3*, respectively. Interestingly, the *SLC45A3-FGFR2* fusion was found in prostate cancer, and exhibits similar expression mechanisms as the other commonly known prostate cancer fusion, *TMPRSS2-ERG/ETV1/ETV4*. Specifically, *FGFR2* is fused to the promoter region of the androgen-driven gene *SLC45A3* (Wu et al, 2013a). *FGFR2* fusions contain the most diverse partner genes, while FGFR3 fusions fuse to only *TACC3* and *BAIAP2L1* genes [reviewed in (Parker et al, 2014)]. Because of the highly diverse array of FGFR family fusions, future efforts should focus on developing FGFR inhibitors that could potentially target several cancer types.

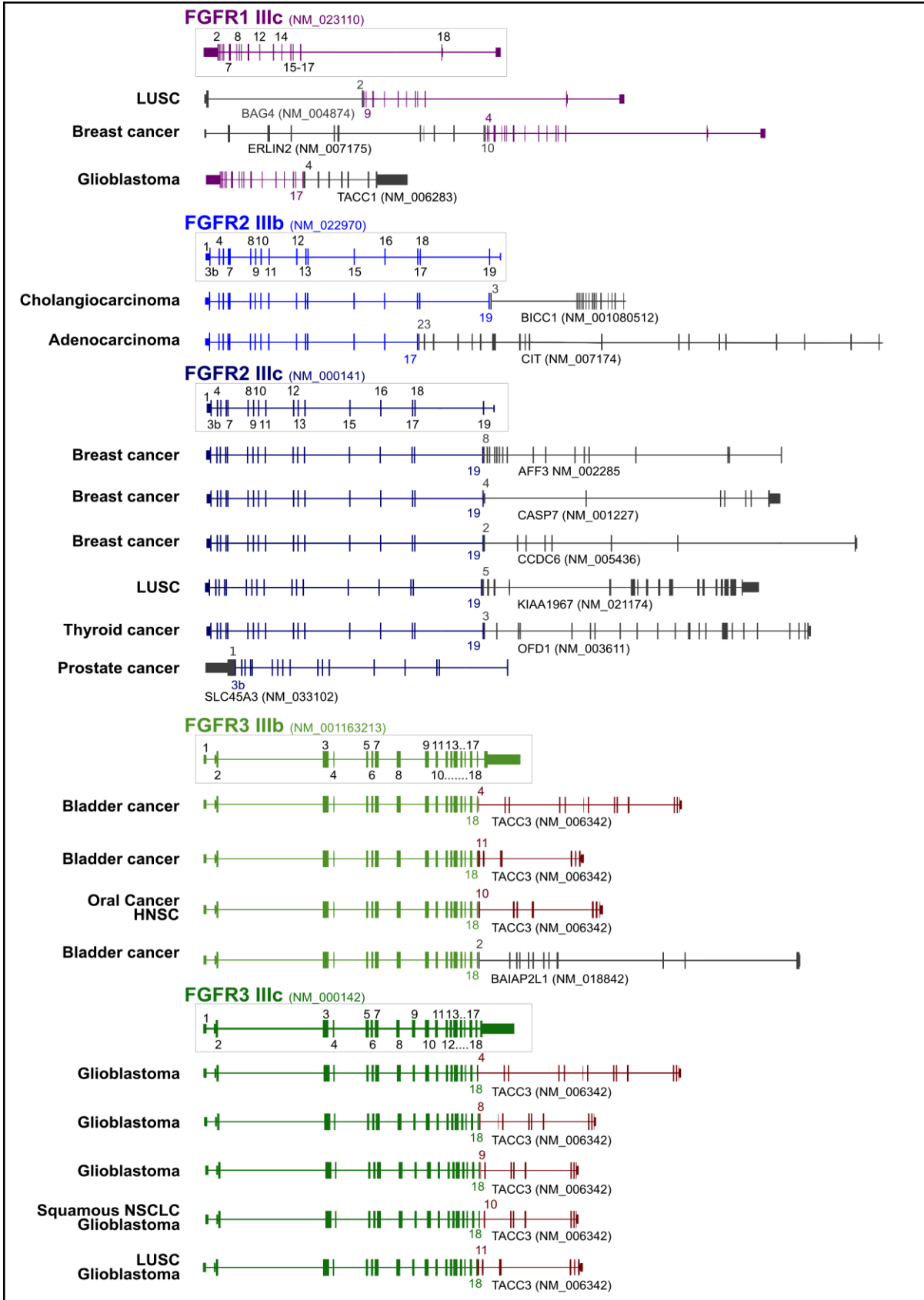


Figure 23. FGFR family fusions occur in a vast array of solid tumors. Included with permission from Parker, B.C., Engels, M., Annala, M., and Zhang, W. (2014). Emergence of FGFR family gene fusions as therapeutic targets in a wide spectrum of solid tumours. *The Journal of pathology* 232, 4-15.

5.2 The *FGFR3-TACC3* fusion is an oncogenic, driver event in GBM.

Both *in vitro* and *in vivo* studies performed by us and others have shown that the *FGFR3-TACC3* fusion is oncogenic (Parker et al, 2013a; Singh et al, 2012). Specifically, the fusion promotes cell proliferation, migration, anchorage-independent cell growth, and is resistant to the frontline chemotherapy agent, TMZ. Fusion-implanted mice exhibited decreased survival *in vivo*, and exhibited high activation of STAT3 and ERK signaling pathways (Parker et al, 2013a). The fusion contains the majority of FGFR3, which sheds light on why the fusion would activate canonical FGFR3 signaling pathways, including ERK and STAT3. However, using primary cell lines, another group found the fusion to inhibit ERK signaling (Singh et al, 2012). TACC3 has also been linked to ERK signaling (Ha et al, 2013b), although it is unlikely that the small portion of TACC3 present within the fusion (coiled-coil domain only) alone promotes this phenotype. The ability of the fusion to promote ERK activity is not limited to GBM alone, but was also found in bladder cancer cell lines as well (Williams et al, 2013a).

Evidence suggests that the presence of the coiled-coil domain promotes ligand-independent activation, as it allows the fusion to dimerize (Wu et al, 2013a). Supporting this hypothesis, we observed ERK activity in serum starved conditions, however we also observed an increase in ERK activity following ligand stimulation, indicating the fusion also responds to ligand treatment (Figure 16A,B). This phenomenon may provide evidence that the fusion can maintain signaling in unfavorable, nutrient-deprived environments that

normally would hinder growth, but can exert an even more aggressive phenotype when nutrients become available.

Genetic instability and heterogeneity are common traits observed in GBM patient samples. Specifically, patients typically exhibit oncogenic gene signatures that co-occur. We sought to determine whether the fusion was mutually exclusive, or existed concurrently with these commonly observed gene signatures. If we found that the fusion typically occurred alongside other genetic events, it could be inferred that the fusion was merely a passenger event to genetic instability. For example, if formation of an oncogene occurred in a region of a chromosome that formed a “hot spot”, and if the genes comprising the fusion were in the same genomic neighborhood, this could suggest a proximal neighbor effect. Interestingly, copy number analysis showed that the fusion was mutually exclusive with commonly amplified genes in GBM, including EGFR, MET, and PDGFRA (Parker et al, 2013a). Furthermore, because the fusion exists in several cancer types (and different cells of origin) further suggests the fusion is not a random passenger event of genetic instability. Therefore, these results suggest that the fusion is not a passenger event, but occurs in isolation to these other known oncogenes, suggesting the fusion itself is a driver event in GBM.

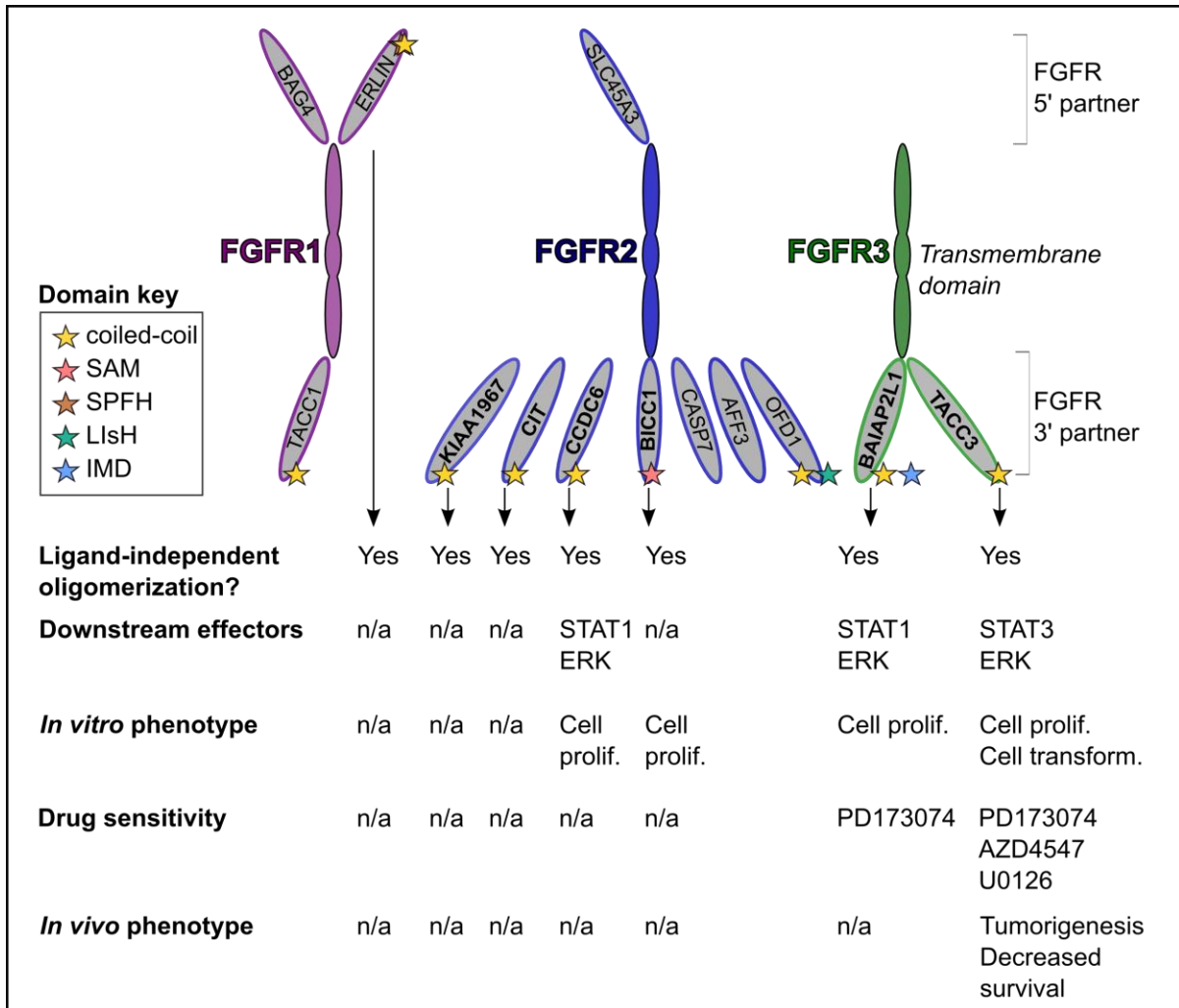


Figure 24. Reported oncogenic phenotypes of FGFR family fusions. Figure used and adapted with permission from Parker, B.C., Engels, M., Annala, M., and Zhang, W. (2014). Emergence of FGFR family gene fusions as therapeutic targets in a wide spectrum of solid tumours. *The Journal of pathology* 232, 4-15.

5.3 The *FGFR3-TACC3* fusion escapes microRNA regulation.

Immunohistochemical and immunoblotting results showed that levels of WT FGFR3 were very low in normal brain and GBM (Figure 8). However, because the fusion contained the majority of FGFR3, and fusion-positive patients exhibited high protein expression, it caused us to question the mechanism as to how the fusion could bypass the negative regulation

that characteristically kept FGFR3 WT levels low (Figure 25). Upon examination of the fusion transcript structure, we noticed that the 3' UTR of FGFR3 was lost upon formation of the fusion. This led us to hypothesize that the fusion was able to bypass the regulation of a particular microRNA that would normally target WT FGFR3. We then performed small RNA sequencing on the same pool of patient samples used to originally discover the fusion, and indeed found a highly expressed miRNA in both GBM and normal brain that was predicted to target FGFR3 WT – miR-99a. We then validated that miR-99a targeted FGFR3 in GBM, and that levels of miR-99a negatively correlated with FGFR3 expression in both GBM and bladder cancer (Figure 9,10). To further show that the fusion is able to bypass miR-99a regulation, we cloned the 3' UTR of FGFR3 onto the coding region of the fusion, and then transfected with either control miRNA or miR-99a. These results confirmed that the fusion was highly expressed because it lacked this microRNA-regulated sequence. The ability of fusion genes to escape microRNA regulation has been described previously in adenoid cystic carcinoma. Specifically, the *MYB-NFIB* fusion is highly expressed because it lost the 3' UTR of *MYB* upon formation of the fusion. Therefore, although WT *MYB* is normally not expressed in these tissues, because this fusion bypasses microRNA regulation, it is overexpressed (Persson et al, 2009).

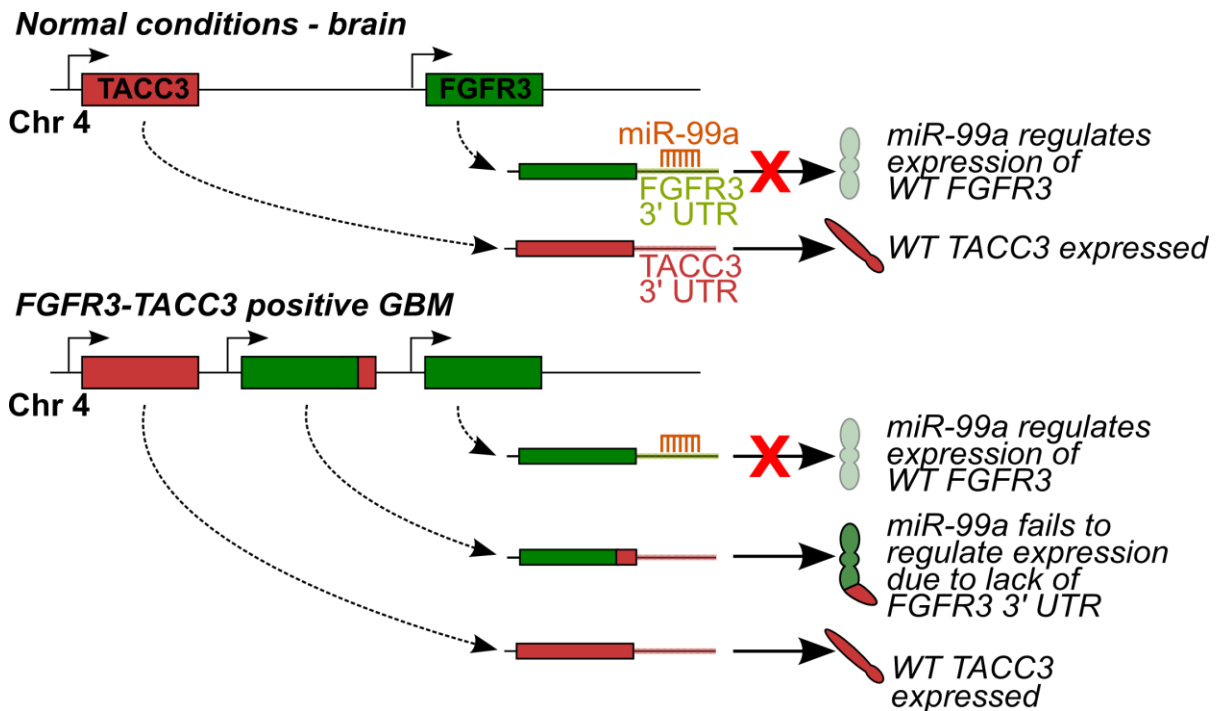


Figure 25. The *FGFR3-TACC3* fusion escapes miR-99a regulation in GBM. Figure used and adapted with permission from Parker, B.C., Engels, M., Annala, M., and Zhang, W. (2014). Emergence of FGFR family gene fusions as therapeutic targets in a wide spectrum of solid tumours. *The Journal of pathology* 232, 4-15.

5.5 Therapeutic implications of targeting the *FGFR3-TACC3* fusion protein.

TMZ is the frontline chemotherapy drug for the treatment of GBM. Therefore, we sought to determine whether fusion expressing cell lines were more sensitive or resistant to TMZ. By performing MTT cell viability and sub G1 apoptosis assays, we determined that the fusion promoted chemoresistance. To gain insight into how the fusion promoted chemoresistance, we looked at differential gene expression in fusion patient samples and cell lines compared to fusion negative samples and cell lines. Because MGMT is normally associated with chemoresistance, we hypothesized that the fusion promoted MGMT expression. However, we found that fusion-positive patients and fusion expressing cell lines did not show a statistically significant increase in MGMT expression.

The fusion was found to promote ERK and STAT3 signaling. Therefore, we sought to determine whether fusion-expressing cell lines would be more sensitive to treatment with FGFR inhibitor PD173074, MEK (ERK) inhibitor U0126, or STAT3 inhibitor WP1066. By performing MTT cell viability assays, we found that fusion cell lines were more sensitive to treatment with these inhibitors. This data suggests that fusion positive patients may benefit from treatment with targeted therapy, but not conventional chemotherapy treatment. Future work will involve determining if these inhibitors or inhibitor combinations are successful in treating fusion-expressing cell lines when they are implanted into the brains of immunocompromised mice.

Because levels of WT FGFR3 are exceedingly low in the brain, treatment with an FGFR3 specific inhibitor for fusion positive patients appears to be an extremely attractive therapeutic option. Because levels of WT FGFR3 are low, this would limit off-target effects as the drug would presumably only target fusion-expressing cancer cells. However, there are no FGFR3-specific inhibitors that are able to cross the blood brain barrier at the present time. Efforts should focus on the development of an FGFR3 specific inhibitor that has the ability to cross the blood brain barrier, to allow for effective drug delivery.

CHAPTER 6: Future directions

6.1 Elucidating the oncogenic result of losing the C-terminal of FGFR3

In both *in vitro* colony formation assays and xenograft glioma models reported by us and others (Parker et al, 2013b; Singh et al, 2012), FGFR3 and TACC3 alone did not show transforming abilities suggesting the fusion of these two proteins confers a gain of oncogenic activity, a paradigm that is commonly accepted. One explanation is that the coiled-coil TACC domain can direct the kinase domain of the FGFR3 portion to some specific compartments of the cell and fire kinase activities in an inappropriate manner. This is supported by our cell fractionation experiments where we showed that the FGFR3-TACC3 protein is abundant in the nucleus in contrast to FGFR3 itself.

Alternatively, deletion of the C-terminal region of FGFR3 may also be functionally important. Recent publications have identified a negative regulatory domain, YLDL, in the C-terminal domain of FGFR family members, which may play a role in receptor trafficking (Cha et al, 2009). In addition, it has been shown that a proline-rich sequence exists in the C-terminal of all FGFR family members that serves as a recruitment site for GRB2 that terminates signaling of the receptor in serum starved conditions (Lin et al, 2012).

We will also examine the oncogenic impact of key phosphorylation sites on FGFR3 that are involved in promoting oncogenesis. We will determine the importance of the FGFR3 C-terminal and TACC domains, as well as phosphorylation sites on the oncogenic activity of the fusion protein by deletion and or mutation of selected regions.

6.2 Determine key phosphorylation sites on *FGFR3-TACC3*

Strong evidence has accumulated over the last two decades suggesting that genomic instability is a hallmark of GBM. GBM is characterized by extensive copy number alterations and point mutations of critical genes. The fact that TACC3 has been shown to be important

for mitosis and can localize to the centrosome suggests that the FGFR3-TACC3 may cause aneuploidy. This hypothesis is supported by the observation that the fusion is localized to spindle poles and delayed mitotic progression leading to defects in chromosomal segregation (Singh et al, 2012). Evidence suggested that fusion-induced aneuploidy was “corrected” upon treatment with pan FGFR inhibitor PD173074 (Singh et al, 2012). The mechanisms through which the fusion protein affected mitosis and chromosomal segregation and the key regulatory switches on FGFR3 are not known. Six phosphorylation sites are conserved across all FGFR family members, four of which are present within the fusion. Both Y647 and Y648 comprise the “activation loop”, whose phosphorylation is required for the conformational changes that accompany receptor activation. Wild-type TACC3 is known as a mitotic regulator that requires the interaction of several binding proteins during mitosis. One such protein is Aurora Kinase A, whose phosphorylation of TACC3 is required for proper localization of TACC3 to centrosomes and mitotic spindles during cell division, and for the recruitment of colonic, hepatic tumor overexpressed gene (ch-TOG) and clathrin to the mitotic spindle (Booth et al, 2011). In fact, evidence suggests that clathrin depletion shows the same phenotypic pattern as TACC3 depletion (Gergely et al, 2003; Royle et al, 2005), and ch-TOG requires Aurora Kinase A mediated activated TACC3 for localization to microtubules (Gergely et al, 2003). Furthermore, deregulation of Aurora A Kinase has been implicated in several cancers and contributes to mitotic abnormality and chromosome instability (Fu et al, 2007) and is overexpressed in GBM and expression is correlated with poor patient prognosis (Figure 2). In this specific aim, we will first test the hypothesis that the TACC domain is responsible for the transportation of the attached FGFR3 kinase domain to the centrosome where it then forms a complex with ch-TOG and Aurora A. In fact, inhibition of Aurora A with the selective small molecule inhibitor MLN8054 resulted in mislocalization of TACC3 and clathrin away from mitotic spindles and microtubules, suggesting that Aurora A Kinase is required for the initial recruitment of

TACC3. Aurora Kinase B, another Aurora kinase family member, has also been implicated in GBM, although to a lesser extent to Aurora Kinase A, and is thought to contribute to the aggressive behavior observed with GBM (Zeng et al, 2007).

Our cell fractionation experiments showed abundant localization of fusion protein in the nucleus. Therefore, it is very likely the fusion protein is not restricted to the centrosome. We propose to investigate whether the fusion protein interacts and regulates other chromosomal segregation machinery proteins that need kinase activation. The candidates for the proteins to study include Aurora A, Aurora B, Cyclin B1, ch-TOG and clathrin. We will carry out protein pull-down experiments to identify the binding proteins.

6.3 Elucidating therapeutic options for *FGFR3-TACC3* patients *in vivo*

GBM is one of the most chemoresistant cancers. A major goal in GBM genomic studies is to identify specific genetic alterations that can be targeted for therapeutics for personalized medicine. Our work and that of our colleagues showed that *FGFR3-TACC* fusion is a recurrent genetic event occurring in up to 8% of GBM patients, and the protein product of this fusion gene is highly expressed in GBM cells due to escape of miR-99a regulation. MiR-99a emerges as a major tumor suppressor miR with an increasing literature report in various cancers. The marked elevation of the fusion protein not only makes it an ideal marker for detection by a simple immunohistochemistry staining in a pathological laboratory, but also makes it a highly specific target for pharmacological inhibition. Several pharmaceutical companies are developing small molecule inhibitors for pan-FGFR that can cross the BBB, and there are efforts in developing *FGFR3*-specific inhibitors. In order to translate this important bench discovery into providing improved patient care, we will test compounds in multiple cell lines using in our xenograft mouse models and most importantly will test them in the spontaneous RCAS glioma model. Currently, the most powerful mouse model for spontaneous glioma development after molecular perturbation is the glial specific RCAS-tva

model, originally developed by Holland in the Varmus laboratory nearly 15 years ago (Holland & Varmus, 1998). Our group has used this model for the past ten years to illustrate that IGFBP2 as a key oncogene in glioma. We will use the RCAS model to complement the xenograft model to test whether expression of the FGFR3-TACC3 fusion may promote gliomagenesis, and possible therapeutics that could be implemented as a therapy for fusion-positive patients. During the course of project, newer drugs that target FGFR3 may emerge and we will have a system in place to test these drugs when they become available. With our system in place, we can also test other drugs such as STAT3 and ERK inhibitors in combination with FGFR inhibitors based on our signaling studies.

CHAPTER 7: Bibliography

Central Brain Tumor Registry of the United States [<http://www.CBTRUS.org>]

(2013) Comprehensive molecular characterization of clear cell renal cell carcinoma. *Nature* **499**: 43-49

Antoniou AC, Spurdle AB, Sinilnikova OM, Healey S, Pooley KA, Schmutzler RK, Versmold B, Engel C, Meindl A, Arnold N, Hofmann W, Sutter C, Niederacher D, Deissler H, Caldes T, Kampjarvi K, Nevanlinna H, Simard J, Beesley J, Chen X, Neuhausen SL, Rebbeck TR, Wagner T, Lynch HT, Isaacs C, Weitzel J, Ganz PA, Daly MB, Tomlinson G, Olopade OI, Blum JL, Couch FJ, Peterlongo P, Manoukian S, Barile M, Radice P, Szabo CI, Pereira LH, Greene MH, Rennert G, Lejbkowitz F, Barnett-Griness O, Andrulis IL, Ozelik H, Gerdes AM, Caligo MA, Laitman Y, Kaufman B, Milgrom R, Friedman E, Domchek SM, Nathanson KL, Osorio A, Llorc G, Milne RL, Benitez J, Hamann U, Hogervorst FB, Manders P, Ligtenberg MJ, van den Ouweland AM, Peock S, Cook M, Platte R, Evans DG, Eeles R, Pichert G, Chu C, Eccles D, Davidson R, Douglas F, Godwin AK, Barjhoux L, Mazoyer S, Sobol H, Bourdon V, Eisinger F, Chompret A, Capoulade C, Bressac-de Paillerets B, Lenoir GM, Gauthier-Villars M, Houdayer C, Stoppa-Lyonnet D, Chenevix-Trench G, Easton DF (2008) Common breast cancer-predisposition alleles are associated with breast cancer risk in BRCA1 and BRCA2 mutation carriers. *American journal of human genetics* **82**: 937-948

Aurias A, Rimbaut C, Buffe D, Dubousset J, Mazabraud A (1983) Chromosomal Translocations in Ewings-Sarcoma. *New Engl J Med* **309**: 496-497

Barros TP, Kinoshita K, Hyman AA, Raff JW (2005) Aurora A activates D-TACC-Msp complexes exclusively at centrosomes to stabilize centrosomal microtubules. *The Journal of cell biology* **170**: 1039-1046

Biesecker JL, Fitch FW, Rowley DA, Stuart FP (1973) Cellular and humoral immunity after allogeneic transplantation in the rat. 3. The effect of passive antibody on cellular and humoral immunity after allogeneic renal transplantation. *Transplantation* **16**: 432-440

Bonaventure J, Horne WC, Baron R (2007) The localization of FGFR3 mutations causing thanatophoric dysplasia type I differentially affects phosphorylation, processing and ubiquitylation of the receptor. *The FEBS journal* **274**: 3078-3093

Booth DG, Hood FE, Prior IA, Royle SJ (2011) A TACC3/ch-TOG/clathrin complex stabilises kinetochore fibres by inter-microtubule bridging. *The EMBO journal* **30**: 906-919

Bralten LB, French PJ (2011) Genetic alterations in glioma. *Cancers* **3**: 1129-1140

Bridge JA, Borek DA, Neff JR, Huntrakoon M (1990) Chromosomal-Abnormalities in Clear Cell-Sarcoma - Implications for Histogenesis. *Am J Clin Pathol* **93**: 26-31

Burton EC, Lamborn KR, Feuerstein BG, Prados M, Scott J, Forsyth P, Passe S, Jenkins RB, Aldape KD (2002) Genetic aberrations defined by comparative genomic hybridization distinguish long-term from typical survivors of glioblastoma. *Cancer research* **62**: 6205-6210

Byron SA, Gartside M, Powell MA, Wellens CL, Gao F, Mutch DG, Goodfellow PJ, Pollock PM (2012) FGFR2 point mutations in 466 endometrioid endometrial tumors: relationship with

MSI, KRAS, PIK3CA, CTNNB1 mutations and clinicopathological features. *PLoS one* **7**: e30801

Camidge DR, Doebele RC (2012) Treating ALK-positive lung cancer--early successes and future challenges. *Nature reviews Clinical oncology* **9**: 268-277

Cancer Genome Atlas Research N (2008) Comprehensive genomic characterization defines human glioblastoma genes and core pathways. *Nature* **455**: 1061-1068

Carpenter G, Cohen S (1990) Epidermal growth factor. *The Journal of biological chemistry* **265**: 7709-7712

Castaigne S, Chomienne C, Daniel MT, Ballerini P, Berger R, Fenaux P, Degos L (1990) All-trans retinoic acid as a differentiation therapy for acute promyelocytic leukemia. I. Clinical results. *Blood* **76**: 1704-1709

Cha JY, Maddileti S, Mitin N, Harden TK, Der CJ (2009) Aberrant receptor internalization and enhanced FRS2-dependent signaling contribute to the transforming activity of the fibroblast growth factor receptor 2 IIIb C3 isoform. *The Journal of biological chemistry* **284**: 6227-6240

Chakraborty J, Okonta H, Bagalab H, Lee SJ, Fink B, Changanamkandath R, Duggan J (2008) Retroviral gene insertion in breast milk mediated lymphomagenesis. *Virology* **377**: 100-109

Cheng S, Douglas-Jones A, Yang X, Mansel RE, Jiang WG (2010) Transforming acidic coiled-coil-containing protein 2 (TACC2) in human breast cancer, expression pattern and clinical/prognostic relevance. *Cancer genomics & proteomics* **7**: 67-73

Chesi M, Nardini E, Brents LA, Schrock E, Ried T, Kuehl WM, Bergsagel PL (1997) Frequent translocation t(4;14)(p16.3;q32.3) in multiple myeloma is associated with increased expression and activating mutations of fibroblast growth factor receptor 3. *Nature genetics* **16**: 260-264

Chin K, DeVries S, Fridlyand J, Spellman PT, Roydasgupta R, Kuo WL, Lapuk A, Neve RM, Qian Z, Ryder T, Chen F, Feiler H, Tokuyasu T, Kingsley C, Dairkee S, Meng Z, Chew K, Pinkel D, Jain A, Ljung BM, Esserman L, Albertson DG, Waldman FM, Gray JW (2006) Genomic and transcriptional aberrations linked to breast cancer pathophysiologies. *Cancer cell* **10**: 529-541

Dailey L, Ambrosetti D, Mansukhani A, Basilico C (2005) Mechanisms underlying differential responses to FGF signaling. *Cytokine & growth factor reviews* **16**: 233-247

Delattre O, Zucman J, Plougastel B, Desmaze C, Melot T, Peter M, Dejong P, Aurias A, Thomas G (1993) Gene Fusion with an Ets Domain Caused by Chromosome-Translocation in Human Tumors. *J Cell Biochem*: 214-214

Dieci MV, Arnedos M, Andre F, Soria JC (2013) Fibroblast growth factor receptor inhibitors as a cancer treatment: from a biologic rationale to medical perspectives. *Cancer discovery* **3**: 264-279

Dreazen O, Klisak I, Jones G, Ho WG, Sparkes RS, Gale RP (1987) Multiple Molecular Abnormalities in Ph1 Chromosome Positive Acute Lymphoblastic-Leukemia. *Brit J Haematol* **67**: 319-374

Duncan CG, Killela PJ, Payne CA, Lampson B, Chen WC, Liu J, Solomon D, Waldman T, Towers AJ, Gregory SG, McDonald KL, McLendon RE, Bigner DD, Yan H (2010) Integrated genomic analyses identify ERRF1 and TACC3 as glioblastoma-targeted genes. *Oncotarget* **1**: 265-277

Dvorak P, Hampl A (2005) Basic fibroblast growth factor and its receptors in human embryonic stem cells. *Folia histochemica et cytobiologica / Polish Academy of Sciences, Polish Histochemical and Cytochemical Society* **43**: 203-208

Ekstrand AJ, James CD, Cavenee WK, Seliger B, Pettersson RF, Collins VP (1991) Genes for epidermal growth factor receptor, transforming growth factor alpha, and epidermal growth factor and their expression in human gliomas in vivo. *Cancer research* **51**: 2164-2172

Fine HA, Dear KB, Loeffler JS, Black PM, Canellos GP (1993) Meta-analysis of radiation therapy with and without adjuvant chemotherapy for malignant gliomas in adults. *Cancer* **71**: 2585-2597

Fu J, Bian M, Jiang Q, Zhang C (2007) Roles of Aurora kinases in mitosis and tumorigenesis. *Mol Cancer Res* **5**: 1-10

Funk JO, Waga S, Harry JB, Espling E, Stillman B, Galloway DA (1997) Inhibition of CDK activity and PCNA-dependent DNA replication by p21 is blocked by interaction with the HPV-16 E7 oncoprotein. *Genes & development* **11**: 2090-2100

Garriga-Canut M, Orkin SH (2004) Transforming acidic coiled-coil protein 3 (TACC3) controls friend of GATA-1 (FOG-1) subcellular localization and regulates the association between GATA-1 and FOG-1 during hematopoiesis. *The Journal of biological chemistry* **279**: 23597-23605

Gergely F, Draviam VM, Raff JW (2003) The ch-TOG/XMAP215 protein is essential for spindle pole organization in human somatic cells. *Genes & development* **17**: 336-341

Gergely F, Karlsson C, Still I, Cowell J, Kilmartin J, Raff JW (2000) The TACC domain identifies a family of centrosomal proteins that can interact with microtubules. *Proceedings of the National Academy of Sciences of the United States of America* **97**: 14352-14357

Gilbert W, Maxam A (1973) The nucleotide sequence of the lac operator. *Proceedings of the National Academy of Sciences of the United States of America* **70**: 3581-3584

Giri D, Ropiquet F, Ittmann M (1999) Alterations in expression of basic fibroblast growth factor (FGF) 2 and its receptor FGFR-1 in human prostate cancer. *Clinical cancer research : an official journal of the American Association for Cancer Research* **5**: 1063-1071

Ha GH, Kim JL, Breuer EK (2013a) Transforming acidic coiled-coil proteins (TACCs) in human cancer. *Cancer letters* **336**: 24-33

Ha GH, Park JS, Breuer EK (2013b) TACC3 promotes epithelial-mesenchymal transition (EMT) through the activation of PI3K/Akt and ERK signaling pathways. *Cancer letters* **332**: 63-73

Hanahan D, Weinberg RA (2011) Hallmarks of cancer: the next generation. *Cell* **144**: 646-674

Hao Z, Stoler MH, Sen B, Shore A, Westbrook A, Flickinger CJ, Herr JC, Coonrod SA (2002) TACC3 expression and localization in the murine egg and ovary. *Molecular reproduction and development* **63**: 291-299

Havrilesky LJ, Alvarez AA, Sayer RA, Lancaster JM, Soper JT, Berchuck A, Clarke-Pearson DL, Rodriguez GC, Carney ME (2003) Weekly low-dose carboplatin and paclitaxel in the treatment of recurrent ovarian and peritoneal cancer. *Gynecologic oncology* **88**: 51-57

Hermanson M, Funa K, Hartman M, Claesson-Welsh L, Heldin CH, Westermark B, Nister M (1992) Platelet-derived growth factor and its receptors in human glioma tissue: expression of messenger RNA and protein suggests the presence of autocrine and paracrine loops. *Cancer research* **52**: 3213-3219

Holland EC, Varmus HE (1998) Basic fibroblast growth factor induces cell migration and proliferation after glia-specific gene transfer in mice. *Proceedings of the National Academy of Sciences of the United States of America* **95**: 1218-1223

Hollstein MC, Metcalf RA, Welsh JA, Montesano R, Harris CC (1990) Frequent mutation of the p53 gene in human esophageal cancer. *Proceedings of the National Academy of Sciences of the United States of America* **87**: 9958-9961

Holzmann K, Grunt T, Heinzle C, Sampl S, Steinhoff H, Reichmann N, Kleiter M, Hauck M, Marian B (2012) Alternative Splicing of Fibroblast Growth Factor Receptor IgIII Loops in Cancer. *Journal of nucleic acids* **2012**: 950508

Huang ME, Ye YC, Chen SR, Chai JR, Lu JX, Zhao L, Gu LJ, Wang ZY (1988) Use of all-trans retinoic acid in the treatment of acute promyelocytic leukemia. *Blood* **72**: 567-572

Hughes SE (1997) Differential expression of the fibroblast growth factor receptor (FGFR) multigene family in normal human adult tissues. *The journal of histochemistry and cytochemistry : official journal of the Histochemistry Society* **45**: 1005-1019

Hughes SE, Crossman D, Hall PA (1993) Expression of basic and acidic fibroblast growth factors and their receptor in normal and atherosclerotic human arteries. *Cardiovascular research* **27**: 1214-1219

Irizarry RA, Hobbs B, Collin F, Beazer-Barclay YD, Antonellis KJ, Scherf U, Speed TP (2003) Exploration, normalization, and summaries of high density oligonucleotide array probe level data. *Biostatistics* **4**: 249-264

Jacinto FV, Esteller M (2007) MGMT hypermethylation: a prognostic foe, a predictive friend. *DNA repair* **6**: 1155-1160

Jakobovits A, Shackelford GM, Varmus HE, Martin GR (1986) Two proto-oncogenes implicated in mammary carcinogenesis, int-1 and int-2, are independently regulated during mouse development. *Proceedings of the National Academy of Sciences of the United States of America* **83**: 7806-7810

Jang JH, Shin KH, Park JG (2001) Mutations in fibroblast growth factor receptor 2 and fibroblast growth factor receptor 3 genes associated with human gastric and colorectal cancers. *Cancer research* **61**: 3541-3543

Jones DT, Kocialkowski S, Liu L, Pearson DM, Backlund LM, Ichimura K, Collins VP (2008) Tandem duplication producing a novel oncogenic BRAF fusion gene defines the majority of pilocytic astrocytomas. *Cancer Res* **68**: 8673-8677

Keats JJ, Reiman T, Maxwell CA, Taylor BJ, Larratt LM, Mant MJ, Belch AR, Pilarski LM (2003) In multiple myeloma, t(4;14)(p16;q32) is an adverse prognostic factor irrespective of FGFR3 expression. *Blood* **101**: 1520-1529

Knezevich SR, McFadden DE, Tao W, Lim JF, Sorensen PHB (1998) A novel ETV6-NTRK3 gene fusion in congenital fibrosarcoma. *Nature genetics* **18**: 184-187

Kroll TG, Sarraf P, Pecciarini L, Chen CJ, Mueller E, Spiegelman BM, Fletcher JA (2000) PAX8-PPARgamma1 fusion oncogene in human thyroid carcinoma [corrected]. *Science* **289**: 1357-1360

Lal S, Lacroix M, Tofilon P, Fuller GN, Sawaya R, Lang FF (2000) An implantable guide-screw system for brain tumor studies in small animals. *Journal of neurosurgery* **92**: 326-333

Langmead B, Trapnell C, Pop M, Salzberg SL (2009) Ultrafast and memory-efficient alignment of short DNA sequences to the human genome. *Genome biology* **10**: R25

Larson RA, Kondo K, Vardiman JW, Butler AE, Golomb HM, Rowley JD (1984) Evidence for a 15;17 translocation in every patient with acute promyelocytic leukemia. *The American journal of medicine* **76**: 827-841

LeRoith D, Roberts CT, Jr. (2003) The insulin-like growth factor system and cancer. *Cancer letters* **195**: 127-137

Li J, Yen C, Liaw D, Podsypanina K, Bose S, Wang SI, Puc J, Miliaresis C, Rodgers L, McCombie R, Bigner SH, Giovanella BC, Ittmann M, Tycko B, Hibshoosh H, Wigler MH, Parsons R (1997) PTEN, a putative protein tyrosine phosphatase gene mutated in human brain, breast, and prostate cancer. *Science* **275**: 1943-1947

Lifshitz B, Fainstein E, Marcelle C, Shtivelman E, Amson R, Gale RP, Canaani E (1988) bcr genes and transcripts. *Oncogene* **2**: 113-117

Lin CC, Melo FA, Ghosh R, Suen KM, Stagg LJ, Kirkpatrick J, Arold ST, Ahmed Z, Ladbury JE (2012) Inhibition of basal FGF receptor signaling by dimeric Grb2. *Cell* **149**: 1514-1524

Manolov G, Manolova Y (1972) Marker Band in One Chromosome-14 from Burkitt Lymphomas. *Nature* **237**: 33-&

Martelli MP, Sozzi G, Hernandez L, Pettirossi V, Navarro A, Conte D, Gasparini P, Perrone F, Modena P, Pastorino U, Carbone A, Fabbri A, Sidoni A, Nakamura S, Gambacorta M, Fernandez PL, Ramirez J, Chan JK, Grigioni WF, Campo E, Pileri SA, Falini B (2009) EML4-ALK rearrangement in non-small cell lung cancer and non-tumor lung tissues. *The American journal of pathology* **174**: 661-670

Moll UM, Petrenko O (2003) The MDM2-p53 interaction. *Molecular cancer research : MCR* **1**: 1001-1008

Moore LM, Kivinen V, Liu Y, Annala M, Cogdell D, Liu X, Liu CG, Sawaya R, Yli-Harja O, Shmulevich I, Fuller GN, Zhang W, Nykter M (2013) Transcriptome and small RNA deep sequencing reveals deregulation of miRNA biogenesis in human glioma. *The Journal of pathology* **229**: 449-459

Murphree AL, Benedict WF (1984) Retinoblastoma: clues to human oncogenesis. *Science* **223**: 1028-1033

Nakamizo A, Marini F, Amano T, Khan A, Studeny M, Gumin J, Chen J, Hentschel S, Vecil G, Dembinski J, Andreeff M, Lang FF (2005) Human bone marrow-derived mesenchymal stem cells in the treatment of gliomas. *Cancer research* **65**: 3307-3318

Nazarenko I, Hede SM, He X, Hedren A, Thompson J, Lindstrom MS, Nister M (2012) PDGF and PDGF receptors in glioma. *Upsala journal of medical sciences* **117**: 99-112

Nordling CO (1953) A new theory on cancer-inducing mechanism. *British journal of cancer* **7**: 68-72

Nowell PC, Hungerford DA (1960) Minute Chromosome in Human Chronic Granulocytic Leukemia. *Science* **132**: 1497-1497

Ohgaki H (2005) Genetic pathways to glioblastomas. *Neuropathology : official journal of the Japanese Society of Neuropathology* **25**: 1-7

Ohgaki H, Kleihues P (2005) Epidemiology and etiology of gliomas. *Acta neuropathologica* **109**: 93-108

Olmos D, Martins AS, Jones RL, Alam S, Scurr M, Judson IR (2011) Targeting the Insulin-Like Growth Factor 1 Receptor in Ewing's Sarcoma: Reality and Expectations. *Sarcoma* **2011**: 402508

Ornitz DM, Itoh N (2001) Fibroblast growth factors. *Genome biology* **2**: REVIEWS3005

Parker BC, Annala MJ, Cogdell DE, Granberg KJ, Sun Y, Ji P, Li X, Gumin J, Zheng H, Hu L, Yli-Harja O, Haapasalo H, Visakorpi T, Liu X, Liu CG, Sawaya R, Fuller GN, Chen K, Lang FF, Nykter M, Zhang W (2013a) The tumorigenic FGFR3-TACC3 gene fusion escapes miR-99a regulation in glioblastoma. *The Journal of clinical investigation* **123**: 855-865

Parker BC, Annala MJ, Cogdell DE, Granberg KJ, Sun Y, Ji P, Li X, Gumin J, Zheng H, Hu L, Yli-Harja O, Haapasalo H, Visakorpi T, Liu X, Liu CG, Sawaya R, Fuller GN, Chen K, Lang FL, Nykter M, Zhang W (2013b) The tumorigenic FGFR3-TACC3 gene fusion escapes miR-99a regulation in glioblastoma. *The Journal of clinical investigation*

Parker BC, Engels M, Annala M, Zhang W (2014) Emergence of FGFR family gene fusions as therapeutic targets in a wide spectrum of solid tumours. *The Journal of pathology* **232**: 4-15

Persson M, Andren Y, Mark J, Horlings HM, Persson F, Stenman G (2009) Recurrent fusion of MYB and NFIB transcription factor genes in carcinomas of the breast and head and neck. *Proceedings of the National Academy of Sciences of the United States of America* **106**: 18740-18744

Piekorz RP, Hoffmeyer A, Duntsch CD, McKay C, Nakajima H, Sexl V, Snyder L, Rehg J, Ihle JN (2002) The centrosomal protein TACC3 is essential for hematopoietic stem cell function and genetically interfaces with p53-regulated apoptosis. *The EMBO journal* **21**: 653-664

Rand V, Huang J, Stockwell T, Ferriera S, Buzko O, Levy S, Busam D, Li K, Edwards JB, Eberhart C, Murphy KM, Tsiamouri A, Beeson K, Simpson AJ, Venter JC, Riggins GJ, Strausberg RL (2005) Sequence survey of receptor tyrosine kinases reveals mutations in glioblastomas. *Proceedings of the National Academy of Sciences of the United States of America* **102**: 14344-14349

Rich JN, Rasheed BK, Yan H (2004) EGFR mutations and sensitivity to gefitinib. *The New England journal of medicine* **351**: 1260-1261; author reply 1260-1261

Rodrigues NR, Rowan A, Smith ME, Kerr IB, Bodmer WF, Gannon JV, Lane DP (1990) p53 mutations in colorectal cancer. *Proceedings of the National Academy of Sciences of the United States of America* **87**: 7555-7559

Rowley JD (1973a) Letter: A new consistent chromosomal abnormality in chronic myelogenous leukaemia identified by quinacrine fluorescence and Giemsa staining. *Nature* **243**: 290-293

Rowley JD (1973b) Letter: Deletions of chromosome 7 in haematological disorders. *Lancet* **2**: 1385-1386

Royle SJ, Bright NA, Lagnado L (2005) Clathrin is required for the function of the mitotic spindle. *Nature* **434**: 1152-1157

Saiki RK, Scharf S, Faloona F, Mullis KB, Horn GT, Erlich HA, Arnheim N (1985) Enzymatic amplification of beta-globin genomic sequences and restriction site analysis for diagnosis of sickle cell anemia. *Science* **230**: 1350-1354

Salzman J, Marinelli RJ, Wang PL, Green AE, Nielsen JS, Nelson BH, Drescher CW, Brown PO (2011) ESRRA-C11orf20 is a recurrent gene fusion in serous ovarian carcinoma. *PLoS biology* **9**: e1001156

Sanger F, Nicklen S, Coulson AR (1977) DNA sequencing with chain-terminating inhibitors. *Proceedings of the National Academy of Sciences of the United States of America* **74**: 5463-5467

Schuster SC (2008) Next-generation sequencing transforms today's biology. *Nat Methods* **5**: 16-18

Scotlandi K, Benini S, Sarti M, Serra M, Lollini PL, Maurici D, Picci P, Manara MC, Baldini N (1996) Insulin-like growth factor I receptor-mediated circuit in Ewing's sarcoma/peripheral neuroectodermal tumor: a possible therapeutic target. *Cancer research* **56**: 4570-4574

Seshagiri S, Stawiski EW, Durinck S, Modrusan Z, Storm EE, Conboy CB, Chaudhuri S, Guan Y, Janakiraman V, Jaiswal BS, Guillory J, Ha C, Dijkgraaf GJ, Stinson J, Gnad F, Huntley MA, Degenhardt JD, Haverty PM, Bourgon R, Wang W, Koeppen H, Gentleman R, Starr TK, Zhang Z, Largaespada DA, Wu TD, de Sauvage FJ (2012) Recurrent R-spondin fusions in colon cancer. *Nature* **488**: 660-664

Shelton JG, Steelman LS, White ER, McCubrey JA (2004) Synergy between PI3K/Akt and Raf/MEK/ERK pathways in IGF-1R mediated cell cycle progression and prevention of apoptosis in hematopoietic cells. *Cell Cycle* **3**: 372-379

Shtivelman E, Lifshitz B, Gale RP, Canaani E (1985a) Fused transcript of abl and bcr genes in chronic myelogenous leukaemia. *Nature* **315**: 550-554

Shtivelman E, Lifshitz B, Gale RP, Canaani E (1985b) Fused Transcript of Abl and Bcr Genes in Chronic Myelogenous Leukemia. *Nature* **315**: 550-554

Silva J, Silva JM, Dominguez G, Garcia JM, Cantos B, Rodriguez R, Larrondo FJ, Provencio M, Espana P, Bonilla F (2003) Concomitant expression of p16INK4a and p14ARF in primary

breast cancer and analysis of inactivation mechanisms. *The Journal of pathology* **199**: 289-297

Singh D, Chan JM, Zoppoli P, Niola F, Sullivan R, Castano A, Liu EM, Reichel J, Porrati P, Pellegatta S, Qiu K, Gao Z, Ceccarelli M, Riccardi R, Brat DJ, Guha A, Aldape K, Golfinos JG, Zagzag D, Mikkelsen T, Finocchiaro G, Lasorella A, Rabadan R, Iavarone A (2012) Transforming fusions of FGFR and TACC genes in human glioblastoma. *Science* **337**: 1231-1235

Sleeman M, Fraser J, McDonald M, Yuan S, White D, Grandison P, Kumble K, Watson JD, Murison JG (2001) Identification of a new fibroblast growth factor receptor, FGFR5. *Gene* **271**: 171-182

Soda M, Choi YL, Enomoto M, Takada S, Yamashita Y, Ishikawa S, Fujiwara S, Watanabe H, Kurashina K, Hatanaka H, Bando M, Ohno S, Ishikawa Y, Aburatani H, Niki T, Sohara Y, Sugiyama Y, Mano H (2007) Identification of the transforming EML4-ALK fusion gene in non-small-cell lung cancer. *Nature* **448**: 561-566

Stupp R, Hegi ME, Mason WP, van den Bent MJ, Taphoorn MJ, Janzer RC, Ludwin SK, Allgeier A, Fisher B, Belanger K, Hau P, Brandes AA, Gijtenbeek J, Marosi C, Vecht CJ, Mokhtari K, Wesseling P, Villa S, Eisenhauer E, Gorlia T, Weller M, Lacombe D, Cairncross JG, Mirimanoff RO (2009a) Effects of radiotherapy with concomitant and adjuvant temozolomide versus radiotherapy alone on survival in glioblastoma in a randomised phase III study: 5-year analysis of the EORTC-NCIC trial. *The lancet oncology* **10**: 459-466

Stupp R, Hegi ME, Mason WP, van den Bent MJ, Taphoorn MJ, Janzer RC, Ludwin SK, Allgeier A, Fisher B, Belanger K, Hau P, Brandes AA, Gijtenbeek J, Marosi C, Vecht CJ, Mokhtari K, Wesseling P, Villa S, Eisenhauer E, Gorlia T, Weller M, Lacombe D, Cairncross JG, Mirimanoff RO, European Organisation for R, Treatment of Cancer Brain T, Radiation Oncology G, National Cancer Institute of Canada Clinical Trials G (2009b) Effects of radiotherapy with concomitant and adjuvant temozolomide versus radiotherapy alone on survival in glioblastoma in a randomised phase III study: 5-year analysis of the EORTC-NCIC trial. *The lancet oncology* **10**: 459-466

Taylor JGt, Cheuk AT, Tsang PS, Chung JY, Song YK, Desai K, Yu Y, Chen QR, Shah K, Youngblood V, Fang J, Kim SY, Yeung C, Helman LJ, Mendoza A, Ngo V, Staudt LM, Wei JS, Khanna C, Catchpoole D, Qualman SJ, Hewitt SM, Merlino G, Chanock SJ, Khan J (2009) Identification of FGFR4-activating mutations in human rhabdomyosarcomas that promote metastasis in xenotransplanted models. *The Journal of clinical investigation* **119**: 3395-3407

Theillet C, Adelaide J, Louason G, Bonnet-Dorion F, Jacquemier J, Adnane J, Longy M, Katsaros D, Sismondi P, Gaudray P, et al. (1993) FGFR1 and PLAT genes and DNA amplification at 8p12 in breast and ovarian cancers. *Genes, chromosomes & cancer* **7**: 219-226

Thut CJ, Goodrich JA, Tjian R (1997) Repression of p53-mediated transcription by MDM2: a dual mechanism. *Genes & development* **11**: 1974-1986

Tomlins SA, Laxman B, Dhanasekaran SM, Helgeson BE, Cao X, Morris DS, Menon A, Jing X, Cao Q, Han B, Yu J, Wang L, Montie JE, Rubin MA, Pienta KJ, Roulston D, Shah RB,

Varambally S, Mehra R, Chinnaiyan AM (2007) Distinct classes of chromosomal rearrangements create oncogenic ETS gene fusions in prostate cancer. *Nature* **448**: 595-599

Tomlins SA, Rhodes DR, Perner S, Dhanasekaran SM, Mehra R, Sun XW, Varambally S, Cao X, Tchinda J, Kuefer R, Lee C, Montie JE, Shah RB, Pienta KJ, Rubin MA, Chinnaiyan AM (2005a) Recurrent fusion of TMPRSS2 and ETS transcription factor genes in prostate cancer. *Science* **310**: 644-648

Tomlins SA, Rhodes DR, Perner S, Dhanasekaran SM, Mehra R, Sun XW, Varambally S, Cao XH, Tchinda J, Kuefer R, Lee C, Montie JE, Shah RB, Pienta KJ, Rubin MA, Chinnaiyan AM (2005b) Recurrent fusion of TMPRSS2 and ETS transcription factor genes in prostate cancer. *Science* **310**: 644-648

Tonon G, Modi S, Wu L, Kubo A, Coxon AB, Komiya T, O'Neil K, Stover K, El-Naggar A, Griffin JD, Kirsch IR, Kaye FJ (2003) t(11;19)(q21;p13) translocation in mucoepidermoid carcinoma creates a novel fusion product that disrupts a Notch signaling pathway (vol 33, pg 208, 2003). *Nature genetics* **33**: 430-430

Turc-Carel C, Dal Cin P, Limon J, Rao U, Li FP, Corson JM, Zimmerman R, Parry DM, Cowan JM, Sandberg AA (1987) Involvement of chromosome X in primary cytogenetic change in human neoplasia: nonrandom translocation in synovial sarcoma. *Proceedings of the National Academy of Sciences of the United States of America* **84**: 1981-1985

Turc-Carel C, Philip I, Berger MP, Philip T, Lenoir G (1983) [Chromosomal translocation (11; 22) in cell lines of Ewing's sarcoma]. *Comptes rendus des seances de l'Academie des sciences Serie III, Sciences de la vie* **296**: 1101-1103

van Rhijn BW, Montironi R, Zwarthoff EC, Jobsis AC, van der Kwast TH (2002) Frequent FGFR3 mutations in urothelial papilloma. *The Journal of pathology* **198**: 245-251

Wang H, Wang H, Shen W, Huang H, Hu L, Ramdas L, Zhou YH, Liao WS, Fuller GN, Zhang W (2003) Insulin-like growth factor binding protein 2 enhances glioblastoma invasion by activating invasion-enhancing genes. *Cancer research* **63**: 4315-4321

Wang SI, Puc J, Li J, Bruce JN, Cairns P, Sidransky D, Parsons R (1997) Somatic mutations of PTEN in glioblastoma multiforme. *Cancer research* **57**: 4183-4186

Weiss J, Sos ML, Seidel D, Peifer M, Zander T, Heuckmann JM, Ullrich RT, Menon R, Maier S, Soltermann A, Moch H, Wagener P, Fischer F, Heynck S, Koker M, Schottle J, Leenders F, Gabler F, Dabow I, Querings S, Heukamp LC, Balke-Want H, Ansen S, Rauh D, Baessmann I, Altmuller J, Wainer Z, Conron M, Wright G, Russell P, Solomon B, Brambilla E, Brambilla C, Lorimier P, Sollberg S, Brustugun OT, Engel-Riedel W, Ludwig C, Petersen I, Sanger J, Clement J, Groen H, Timens W, Sietsma H, Thunnissen E, Smit E, Heideman D, Cappuzzo F, Ligorio C, Damiani S, Hallek M, Beroukhi R, Pao W, Klebl B, Baumann M, Buettner R, Ernestus K, Stoelben E, Wolf J, Nurnberg P, Perner S, Thomas RK (2010) Frequent and focal FGFR1 amplification associates with therapeutically tractable FGFR1 dependency in squamous cell lung cancer. *Science translational medicine* **2**: 62ra93

Williams SV, Hurst CD, Knowles MA (2013a) Oncogenic FGFR3 gene fusions in bladder cancer. *Human molecular genetics* **22**: 795-803

Williams SV, Hurst CD, Knowles MA (2013b) Oncogenic FGFR3 gene fusions in bladder cancer. *Hum Mol Genet* **22**: 795-803

Wu CL, Zukerberg LR, Ngwu C, Harlow E, Lees JA (1995) In vivo association of E2F and DP family proteins. *Molecular and cellular biology* **15**: 2536-2546

Wu X, Bayle JH, Olson D, Levine AJ (1993) The p53-mdm-2 autoregulatory feedback loop. *Genes & development* **7**: 1126-1132

Wu YM, Su F, Kalyana-Sundaram S, Khazanov N, Ateeq B, Cao X, Lonigro RJ, Vats P, Wang R, Lin SF, Cheng AJ, Kunju LP, Siddiqui J, Tomlins SA, Wyngaard P, Sadis S, Roychowdhury S, Hussain MH, Feng FY, Zalupski MM, Talpaz M, Pienta KJ, Rhodes DR, Robinson DR, Chinnaiyan AM (2013a) Identification of targetable FGFR gene fusions in diverse cancers. *Cancer discovery* **3**: 636-647

Wu YM, Su F, Kalyana-Sundaram S, Khazanov N, Ateeq B, Cao X, Lonigro RJ, Vats P, Wang R, Lin SF, Cheng AJ, Kunju LP, Siddiqui J, Tomlins SA, Wyngaard P, Sadis S, Roychowdhury S, Hussain MH, Feng FY, Zalupski MM, Talpaz M, Pienta KJ, Rhodes DR, Robinson DR, Chinnaiyan AM (2013b) Identification of Targetable FGFR Gene Fusions in Diverse Cancers. *Cancer discovery*

Yoshida T, Tsutsumi M, Sakamoto H, Miyagawa K, Teshima S, Sugimura T, Terada M (1988) Expression of the HST1 oncogene in human germ cell tumors. *Biochemical and biophysical research communications* **155**: 1324-1329

Zammit C, Barnard R, Gomm J, Coope R, Shousha S, Coombes C, Johnston C (2001) Altered intracellular localization of fibroblast growth factor receptor 3 in human breast cancer. *The Journal of pathology* **194**: 27-34

Zeng WF, Navaratne K, Prayson RA, Weil RJ (2007) Aurora B expression correlates with aggressive behaviour in glioblastoma multiforme. *Journal of clinical pathology* **60**: 218-221

CHAPTER 8: Vita

Brittany Candies Parker Kerrigan was born in Torrance, California on August 23, 1985, the daughter of Barbara Reich Parker and Steven Uzelac Parker, Sr. She completed her work at The University of California, Irvine in 2008, where she earned a degree of Bachelor of Science with a major in Biology. For the next year and a half, she worked as a Biology Professional in the Department of Retinal Disease at Allergan, Inc. located in Irvine, California. In September of 2009 she entered The University of Texas Graduate School of Biomedical Sciences at Houston.